CMS-SMP-14-023

arXiv:1610.04222v1 [hep-ex] 13 Oct 2016

Measurements of differential cross sections for associated production of a W boson and jets in proton-proton collisions at $\sqrt{s} = 8\,\text{TeV}$

The CMS Collaboration[*]

Abstract

Differential cross sections for a W boson produced in association with jets are measured in a data sample of proton-proton collisions at a center-of-mass energy of 8 TeV recorded with the CMS detector and corresponding to an integrated luminosity of $19.6\,\text{fb}^{-1}$. The W bosons are identified through their decay mode $W \to \mu\nu$. The cross sections are reported as functions of jet multiplicity, transverse momenta, and the scalar sum of jet transverse momenta (H_T) for different jet multiplicities. Distributions of the angular correlations between the jets and the muon are examined, as well as the average number of jets as a function of H_T and as a function of angular variables. The measured differential cross sections are compared with tree-level and higher-order recent event generators, as well as next-to-leading-order and next-to-next-to-leading-order theoretical predictions. The agreement of the generators with the measurements builds confidence in their use for the simulation of W+jets background processes in searches for new physics at the LHC.

[*]See Appendix A for the list of collaboration members

1   Introduction

This paper presents measurements of differential cross sections for associated production of a W boson and jets in proton-proton collisions at a center-of-mass energy of 8 TeV at the CERN LHC. Measurements of the production of vector bosons in association with jets provide stringent tests of perturbative quantum chromodynamics (QCD). In addition, the production of a W boson in association with jets (W+jets) is the main background source for rarer standard model (SM) processes, such as top quark production and Higgs boson production in association with a W boson, and it is also a prominent background to several searches for physics beyond the SM.

The studies described here focus on the production of W+jets with the subsequent decay of the W boson into a muon and a neutrino. The final-state topology is characterized by one isolated muon with high transverse momentum p_T, significant missing transverse energy E_T^{miss}, and up to seven jets. Because of higher trigger thresholds and additional systematic uncertainties, the decay channel of the W boson into an electron and a neutrino is not considered. Differential cross sections are extracted as functions of jet multiplicity, the p_T of the jets, the scalar sum of the jet transverse momenta, H_T, and the pseudorapidity η of the jets. Measurements of differential cross sections as functions of angular correlation variables are also performed. The average number of jets per event, $\langle N_{jets} \rangle$, is further studied as a function of H_T and angular variables.

These measurements are based on a sample of proton-proton collisions at $\sqrt{s} = 8$ TeV recorded with the CMS detector, corresponding to an integrated luminosity of 19.6 fb^{-1}. In order to perform differential measurements of the W+jets cross section, a high-purity sample of muonic W boson decays is selected and the distributions are corrected back to the stable-particle level by means of a regularized unfolding procedure. The measured fiducial differential cross sections are compared to the predictions of Monte Carlo (MC) event generators for the $W + n$ jets hard-scattering process, with final states of different parton multiplicities matched to parton showers. The generators used are MADGRAPH 5 [1] interfaced with PYTHIA [2], which uses a leading-order (LO) matrix element calculation, and MADGRAPH5_aMC@NLO [3] and SHERPA 2 [4], which use next-to-leading-order (NLO) matrix element calculations. The differential cross sections are also compared with the NLO parton-level predictions of BLACK-HAT+SHERPA [5] and with a next-to-next-to-leading-order (NNLO) calculation for the production of $W + 1$ jet [6, 7].

Previous measurements of W+jets production were performed by the CDF [8] and D0 [9, 10] Collaborations in proton-antiproton collisions at $\sqrt{s} = 1.96$ TeV at the Fermilab Tevatron. The ATLAS [11] and CMS [12] Collaborations have measured W+jets production cross sections in proton-proton collisions at $\sqrt{s} = 7$ TeV at the LHC, corresponding to integrated luminosities of 4.6 and 5.0 fb^{-1}, respectively.

The differential W+jets cross sections at 8 TeV presented in this paper extend the kinematic reach of the 7 TeV CMS results (in p_T, H_T, and jet multiplicity) and expand the set of kinematic observables studied. The increased center-of-mass energy widens the observed ranges of kinematic quantities, such as the p_T of the jets in the event and H_T for higher jet multiplicities, that are sensitive to higher-order processes. The larger data sample motivates the increase in number and complexity of the angular correlation variables examined to more accurately understand how particle emissions are modeled by the MC generators used in the analysis of the LHC data and by the most current NLO calculations. The quantity $\langle N_{jets} \rangle$ is studied as a function of H_T and angular correlation variables to further explore the modeling of higher-order processes and correlations among emitted particles. In addition, the measurements are expanded to include the cross section dependence on variables, such as the dijet invariant mass

in different multiplicity ranges, that are sensitive to the presence of physics beyond the SM.

This paper is organized in the following manner: Section 2 describes the CMS detector. Section 3 describes the MC simulated samples and the data sample used for the analysis. The identification criteria for the final-state objects and the selection criteria used to select $W(\to \mu\nu)$+jets events are listed in Section 4. Section 5 describes the modeling of the backgrounds. The variables used for the differential cross section measurements are detailed in Section 6. The procedure used for unfolding is detailed in Section 7, and Section 8 describes the systematic uncertainties. Finally, Section 9 gives the results and Section 10 summarizes them.

2   The CMS detector

The CMS detector consists of an inner tracking system and electromagnetic (ECAL) and hadron (HCAL) calorimeters surrounded by a 3.8 T superconducting solenoid. The inner tracking system consists of a silicon pixel and strip tracker, providing the required granularity and precision for the reconstruction of vertices of charged particles in the range $0 < \phi < 2\pi$ in azimuth and $|\eta| < 2.5$ in pseudorapidity. The crystal ECAL and the brass and scintillator HCAL are used to measure with high resolution the energies of photons, electrons, and hadrons for $|\eta| < 3.0$. The three muon systems surrounding the solenoid cover the region $|\eta| < 2.4$ and are composed of drift tubes in the barrel region ($|\eta| < 1.2$), cathode strip chambers in the endcaps ($0.9 < |\eta| < 2.4$), and resistive plate chambers in both the barrel region and the endcaps ($|\eta| < 1.6$). Events are recorded based on a trigger decision using information from the CMS detector subsystems. The first level of the trigger system, composed of custom hardware processors, uses information from the calorimeters and muon detectors to select events in a fixed time interval of less than 4 μs. The final trigger decision is based on the information from all subsystems, processed by the high-level trigger (HLT), which consists of a farm of computers running a version of the reconstruction software optimized for fast processing. The HLT processor farm decreases the event rate from 100 kHz to less than 1 kHz, before data storage. A more detailed description of the CMS detector, together with a definition of the coordinate system used and the relevant kinematic variables, can be found in Ref. [13].

3   Data and simulated samples

Events are retained if they pass a trigger selection requiring one isolated muon with $p_{\mathrm{T}} > 24$ GeV and $|\eta| < 2.1$.

Signal and background processes are generated with various state-of-the-art generators and passed through detector simulation based on GEANT4 [14] description of CMS. Subsequently reconstructed samples are used for analysis to study various aspects of the events. Each simulated sample is normalized to the integrated luminosity of the data sample. The simulated events are required to pass an emulation of the trigger requirements applied to the data. Trigger efficiencies in the simulation are corrected for differences with respect to the data. Simulations also include additional collisions in the same or adjacent bunch crossings (pileup, PU). To model PU, minimum-bias events generated with PYTHIA6 using the Z2* tune [15] are superimposed on the simulated events, matching the multiplicity of PU collisions observed in data, which has an average value of approximately 21.

The W+jets signal process is simulated with the matrix element (ME) generator MADGRAPH 5.1.1 [1] interfaced with PYTHIA 6.426 using the Z2* tune for parton showering and hadronization. This sample of events, denoted MADGRAPH5+PYTHIA6 (denoted as MG5+PY6 in the

figure legends), is produced with the CTEQ6L1 parton distribution function (PDF) set [16] and is normalized to the inclusive NNLO cross section calculated with FEWZ 3.1 [17]. The MADGRAPH5+PYTHIA6 calculation includes the production of up to four partons at LO. The jets from matrix elements are matched to parton showers following the k_T-jet MLM prescription [18], where partons are clustered using the k_T algorithm [19] with a distance parameter of 1. The merging of parton showers and matrix elements with the MLM scheme uses a matching scale of 20 GeV. The factorization and renormalization scales for the 2→2 hard process in the event are chosen to be the transverse mass of the W boson produced in the central process. The k_T computed for each QCD emission vertex is used as renormalization scale for the calculation of the strong coupling constant α_S of that vertex.

Background processes include $t\bar{t}$, single top quark, Z/γ^*+jets, diboson (ZZ/WZ/WW) + jets, and QCD multijet production. Their contributions, with the exception of QCD multijet production, are estimated from simulation. The simulated samples of $t\bar{t}$ and Z/γ^*+jets events are generated with MADGRAPH version 5.1.1; the single top quark samples (s-, t-, and tW-channel production) are generated with POWHEG version 1 [20–23]; and the diboson samples (WW, WZ, or ZZ) are generated with PYTHIA 6.424 using the Z2* tune. The simulations with MADGRAPH and PYTHIA use the CTEQ6L1 PDFs, and the simulations with POWHEG use the CTEQ6M PDFs. The Z/γ^*+jets sample is normalized to the NNLO inclusive cross section calculated with FEWZ 3.1 [17]. Single top quark and diboson samples are normalized to NLO inclusive cross sections calculated with MCFM [24–27]. The $t\bar{t}$ contribution is normalized to the predicted cross section at NNLO with next-to-next-to-leading-logarithm accuracy [28].

When comparing the measurements with the theoretical prediction, other event generators are used for the W+jets process. Those generators, which are not used for the measurement itself, are described in Section 9.

4 Object identification and event selection

The final-state particles in W+jets events are identified and reconstructed with the particle-flow (PF) algorithm [29, 30], which optimally combines the information from the various elements of the CMS detector.

Muon PF candidates are reconstructed as tracks in the muon system that are matched to tracks reconstructed in the inner tracking system [31]. Muons are required to have $p_T > 25$ GeV and to be reconstructed in the HLT fiducial volume $|\eta| < 2.1$. The track associated with a muon candidate is required to have hits in at least six strip tracker layers, at least one pixel hit, segments from at least two muon stations, and a good quality global fit with χ^2 per degree of freedom < 10. In order to reduce the contamination due to muons that do not originate from the decay of a W boson, an isolation requirement is imposed:

$$I_{\text{iso}} = \frac{1}{p_T^\mu} \left[\sum^{\text{charged}} p_T + \max\left(0, \sum^{\text{neutral}} p_T + \sum^{\gamma} p_T - 0.5 \sum^{\text{PU}} p_T \right) \right] \leq 0.12, \quad (1)$$

where the sums run over charged hadrons originating from the primary vertex of the event, neutral hadrons, photons (γ), and charged hadrons not originating from the primary vertex but from PU; only PF candidates with direction within a cone defined by $\Delta R = \sqrt{(\Delta\phi)^2 + (\Delta\eta)^2} < 0.4$ around the direction of the muon candidate track are considered. The transverse momentum of the muon candidate is denoted by p_T^μ. Because neutral PU particles deposit on average half as much energy as charged PU particles, the contamination in the isolation cone from neu-

tral particles coming from PU interactions is estimated as $0.5 \sum^{\mathrm{PU}} p_{\mathrm{T}}$ and it is subtracted in the definition of I_{iso}.

To reject muons from cosmic rays, the transverse impact parameter of the muon candidate with respect to the primary vertex is required to be less than 2 mm, and the longitudinal distance of the tracker track from the primary vertex is required to be less than 5 mm. Trigger efficiency corrections, as well as muon identification and isolation efficiency corrections, are applied to the simulation as a function of p_{T} and η on an event-by-event basis and are generally less than 4% and 2.5%, respectively.

Jets and transverse missing energy $E_{\mathrm{T}}^{\mathrm{miss}}$ are also reconstructed using the PF algorithm. The missing momentum vector $\vec{p}_{\mathrm{T}}^{\,\mathrm{miss}}$ of an event is defined as the negative of the vectorial p_{T} sum of the particles reconstructed with the PF algorithm; $E_{\mathrm{T}}^{\mathrm{miss}}$ is defined as the magnitude of the $\vec{p}_{\mathrm{T}}^{\,\mathrm{miss}}$ vector. Jets are reconstructed using the anti-k_{T} [19, 32] algorithm with a distance parameter of 0.5. Reconstructed jet energies are corrected with p_{T}- and η-dependent correction factors to account for the following effects: nonuniformity and nonlinearity of the ECAL and HCAL energy response to neutral hadrons, the presence of extra particles from PU interactions, the thresholds used in jet constituent selection, reconstruction inefficiencies, and possible biases introduced by the clustering algorithm. Jet energy corrections are derived from simulation and adjusted using measurements of the p_{T} balance in dijet and γ+jet events [33]. The jet energy resolution is approximately 15% at 10 GeV, 8% at 100 GeV, and 4% at 1 TeV [33]. Jets are required to have $p_{\mathrm{T}} > 30$ GeV, $|\eta| < 2.4$, and a spatial separation from muon candidates of $\Delta R > 0.5$. In order to reduce the contamination from PU, jets are required to be matched to the same primary vertex as the muon candidate.

The primary background process for the measurement of W+jets at high jet multiplicities (4 or more) is $t\bar{t}$ production. To reduce the $t\bar{t}$ contamination, a veto is applied that removes events containing one or more b-tagged jets. The tagging criteria used for this veto are based on the combined secondary vertex algorithm (CSV) [34], which exploits the long lifetime of b hadrons by combining information about impact parameter significance, secondary vertices, and jet kinematic properties. Differences in the b tagging efficiency in data and simulation, as well as differences in mistagging rates, are corrected using scale factors [34] determined as a function of p_{T} in multijet and $t\bar{t}$ events. Specifically, the tagging efficiency in simulation is decreased by randomly untagging b-tagged jets such that the data and simulated efficiencies are matched. Additionally, a small adjustment to the mistagging rates is performed by randomly tagging untagged jets in simulated events such that the data and simulated mistagging rates agree within uncertainties.

In order to select a $W(\to \mu\nu)$+jets sample, events are required to contain exactly one muon satisfying the muon selection criteria described above and one or more jets with $p_{\mathrm{T}} > 30$ GeV. Events containing additional muons with $p_{\mathrm{T}} > 15$ GeV are vetoed. Events are required to have $M_{\mathrm{T}} > 50$ GeV, where M_{T}, the transverse mass of the muon and missing transverse energy, is defined as $M_{\mathrm{T}} = \sqrt{2 p_{\mathrm{T}}^{\mu} E_{\mathrm{T}}^{\mathrm{miss}} (1 - \cos \Delta\phi)}$ and $\Delta\phi$ is the difference in the azimuthal angle between the direction of the muon momentum and $\vec{p}_{\mathrm{T}}^{\,\mathrm{miss}}$.

5 Estimation of the backgrounds

Leptonic W boson decays are characterized by a prompt, energetic, isolated lepton and a neutrino giving rise to significant $E_{\mathrm{T}}^{\mathrm{miss}}$. Background processes with final-state signatures similar to that of W+jets are $t\bar{t}$, single top quark, Z+jets, diboson (ZZ/WZ/WW)+jets, and QCD multijet production. All background processes except for QCD multijet production are simulated by

MC event generators and are normalized as described in Section 3.

The multijet background is estimated using a control data sample with an inverted muon isolation requirement. In the control data sample, the muon misidentification rate is estimated in a multijet-enriched sideband region with $M_T < 50$ GeV, and the shape of the multijet distribution is determined in the region with $M_T > 50$ GeV. The template for the multijet shape is rescaled according to the muon misidentification rate. This method of estimation was used in the measurement of the W+jets fiducial cross sections at 7 TeV and is described in detail in Ref. [12].

The dominant source of background comes from the $t\bar{t}$ process, which is reduced by the application of the b jet veto described in Section 4. For jet multiplicities of 1 to 7, the b jet veto rejects 62–88% of the predicted $t\bar{t}$ background, while eliminating 4–22% of the predicted W+jets signal.

6   Measured observables

Fiducial cross sections are measured as a function of jet multiplicity, inclusively and exclusively, as a function of jet p_T and $|\eta|$, and as a function of H_T. In terms of angular correlations between jets, cross sections are measured as a function of the difference in rapidity $\Delta y(j_i, j_k)$, and of the difference in azimuthal angle $\Delta\phi(j_i, j_k)$, between the ith and kth jets from the p_T-ordered list of jets in the event. Cross sections are also measured as a function of the differences in rapidity and in azimuthal angle between rapidity-ordered jets, most notably $\Delta y(j_F, j_B)$ and $\Delta\phi(j_F, j_B)$, the differences between the most forward and the most backward jet in the event. Cross sections are measured as a function of $\Delta R(j_1, j_2) = \sqrt{\Delta\phi(j_1, j_2)^2 + \Delta y(j_1, j_2)^2}$ between p_T-ordered jets. The dependence of the cross section on the invariant mass of the two leading jets for different jet multiplicities is also examined. The difference in azimuthal angle between the muon and the leading jet is measured for different jet multiplicities. The dependence of $\langle N_{jets} \rangle$ on H_T and on both $\Delta y(j_1, j_2)$ and $\Delta y(j_F, j_B)$ is studied for different jet multiplicities.

Before correcting for detector effects and determining the cross section values, we compare the kinematic distributions reconstructed in data with the predictions for the simulated W+jets signal and the simulated background processes. The comparison of reconstructed data and simulated signal and background processes is shown in Fig. 1 for the inclusive jet multiplicity. The uncertainty band represents the total statistical and systematic uncertainty including uncertainties in the jet energy scale and resolution, the muon momentum scale and resolution, the integrated luminosity, the pileup modeling, the normalizations of the background processes, the modeling of the Wb contribution in the signal simulation, and the reconstruction, identification, and trigger efficiencies.

The number of events in each bin of exclusive reconstructed jet multiplicity for both data and simulated signal and backgrounds is listed in Table 1. The predicted total yields agree well with the data yields for all the values of jet multiplicity.

7   Unfolding procedure

The fiducial cross sections are obtained by subtracting the simulated backgrounds and the estimated multijet background from the data distributions and correcting the background-subtracted data distributions back to the particle level using an unfolding procedure. This procedure takes detector effects such as detection efficiency and resolution into account. The unfolding procedure is performed using the iterative d'Agostini method [35] implemented in

Table 1: Number of events in data and simulation as a function of exclusive reconstructed jet multiplicity. The purity is the number of simulated signal events (W+jets) divided by the total number of simulated signal and background events (Total). The ratio is the total number of simulated signal and background events divided by the number of data events.

N_{jets}	0	1	2	3	4	5	6	≥ 7
WW+jets	18 093	24 420	13 472	3057	515	77	12	1
WZ+jets	8125	6799	4153	1042	183	30	4	0
ZZ+jets	932	669	384	96	18	3	0	0
QCD multijet	570 722	228 188	37 154	6734	1076	171	40	9
Single top quark	6438	14 386	9838	3444	877	196	34	7
Z/γ+jets	1 935 191	265 387	51 613	9570	1697	281	48	6
$t\bar{t}$	1504	7576	16 052	17 377	10 090	3487	1000	288
W+jets	54 617 816	6 999 393	1 320 381	222 457	37 822	5857	860	139
Total	57 158 821	7 546 818	1 453 047	263 777	52 278	10 102	1998	450
Purity	0.96	0.93	0.91	0.84	0.72	0.58	0.43	0.31
Data	57 946 098	7 828 967	1 517 517	279 678	54 735	10 810	2058	441
Ratio	0.99	0.96	0.96	0.94	0.96	0.93	0.97	1.02
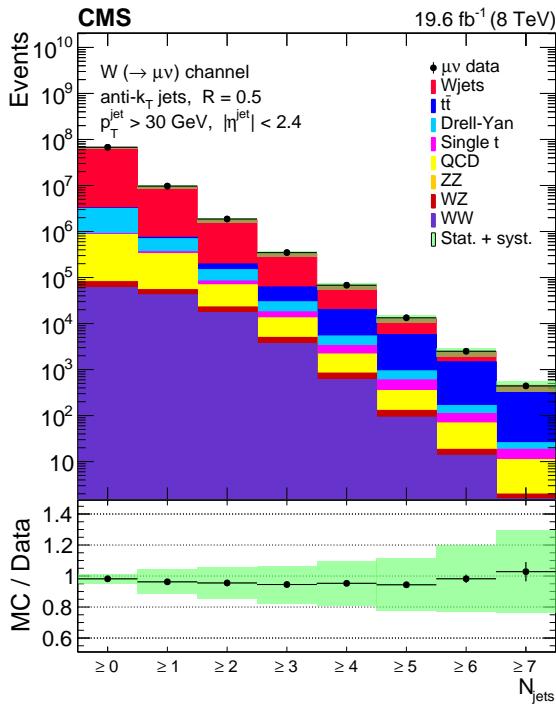
Figure 1: Distribution of inclusive jet multiplicity, for reconstructed data (points) and simulated signal and backgrounds (histograms). The ratio of simulated and measured data events is shown below the distribution. The data points are shown with statistical error bars. The error band represents the total statistical and systematic uncertainty.

the RooUnfold toolkit [36]. Regularization is achieved by choosing the optimal value of number of iterations. To assess the dependence of the results on the unfolding method, we also used the singular-value decomposition method [37]. The results from the two methods agree within the uncertainties.

A response matrix, which defines the probability of event migration between the particle-level and reconstructed phase space as well as the overall reconstruction efficiency, is constructed using a W+jets sample simulated with MADGRAPH5+PYTHIA6. The particle-level selection defines the fiducial phase space of the measurements and is identical to the selection applied to the reconstructed objects, including the requirement of exactly one muon with $p_T > 25$ GeV and $|\eta| < 2.1$, jet $p_T > 30$ GeV and $|\eta| < 2.4$, and $M_T > 50$ GeV. The particle-level E_T^{miss} is determined using the neutrino from the decay of the W boson. The momenta of all photons in a cone of $\Delta R < 0.1$ around the muon are added to that of the muon in order to take into account final-state radiation. The particle-level jets are clustered using the anti-k_T [32] algorithm with a distance parameter of 0.5. The jet clustering algorithm uses all particles after decay and fragmentation, excluding neutrinos. The b jet veto explained in Section 4 is treated as an overall event selection requirement, and the cross section is corrected by the unfolding procedure to correspond to W boson production in association with jets of any flavor. The contribution from $W \rightarrow \tau \nu$ decays resulting in a muon in the final state is estimated to be small ($\sim$1% of selected signal sample), and it is therefore not considered as part of the signal definition at the particle level.

8 Systematic uncertainties

The systematic uncertainties are evaluated by repeating all of the analysis steps (including the subtraction of backgrounds and unfolding) with systematic variations corresponding to the different sources of uncertainty. The difference in each bin between the results obtained with and without the variation is taken as the systematic uncertainty.

The dominant systematic uncertainties are those associated with the jet energy scale (JES) and jet energy resolution (JER). The JES uncertainty is propagated to the cross section measurements by varying the jet p_T scale in data by the magnitude of the uncertainty, which is parametrized as a function of p_T and η [33]. Shifting the value of p_T for each individual jet affects E_T^{miss}, therefore E_T^{miss} is recalculated. This variation also affects the value of M_T, which is used in the event selection. The uncertainties related to JER are assessed by varying within their uncertainties the calibration factors applied to the simulation to reproduce the resolution observed in data [33]. As in the case of JES, the changes in jet p_T due to JER are propagated to the calculation of E_T^{miss} and M_T.

An uncertainty of 0.2% in the muon momentum scale and an uncertainty of 0.6% in muon momentum resolution are assigned [31]. The effects of these uncertainties on the measured cross sections are evaluated by varying the momentum scale and by fluctuating the muon momentum in the simulation.

The systematic uncertainty associated with the generator used to build the unfolding response matrix is assessed by weighting the simulation to agree with the data in each distribution and constructing an alternative response matrix to unfold the data. The difference between the unfolded results obtained using the weighted response matrix and the nominal results is taken as the systematic uncertainty associated with the unfolding response matrix. For the leading jet p_T cross section, the resulting uncertainty is in the range 0.02–10.8%. The higher values in this range, as well as in other uncertainty ranges, are caused by statistical fluctuations in the

data and simulation samples in certain kinematic regions.

Other sources of systematic uncertainty include the normalization of the background processes; b tagging efficiency; modeling of the Wb contribution in the signal simulation; integrated luminosity; PU modeling; muon trigger, isolation, and identification criteria; and the finite number of simulated events used to build the response matrix.

Background normalization uncertainties are determined by varying the cross sections of the backgrounds within their theoretical uncertainties [24–27, 38]. The theoretical cross section uncertainties are 6% for ZZ and WZ, 8% for WW, and 4% for Z+jets for the region $M_{\mu\mu} > 50\,\text{GeV}$. For single top quark production, the uncertainties are 6% for the s and t channels and 9% for the tW channel. The uncertainty in the $t\bar{t}$ modeling is assessed by comparing data and simulation in a data control region with two or more b-tagged jets. Simulated events are rescaled to match data in the control region, and the difference in the unfolded results with or without rescaling applied is taken as the systematic uncertainty related to $t\bar{t}$ modeling. The scale factors are about 1.26 for jet multiplicity of 2, and between 1.0 and 1.1 for jet multiplicities larger than 2, leading to uncertainties in the measured cross sections that range from 0.4% to 27% for jet multiplicities of 2 to 7. The estimate of the multijet background has an uncertainty based on the number of events in the inverted isolation sample and in the control regions where the normalization of the multijet background is calculated. In addition, the systematic variations applied to the backgrounds in the multijet control regions introduce variations in the multijet normalization and shape.

Uncertainties in the ratio of the b tagging efficiencies in data and simulation are estimated [39], leading to uncertainties in the measured cross sections in the range 0.4% to 25% for jet multiplicities of 1 to 7.

The uncertainty related to the normalization of the Wb content in the signal is estimated by examining the agreement between data and simulation as a function of jet multiplicity in a control region defined by requiring exactly one b-tagged jet. The normalization of Wb production is found to be underestimated in the simulation by a factor of 1.3. Enhancing the Wb process in simulation by this factor leads to an estimated uncertainty in the measurement of up to 0.8% for a jet multiplicity of 7.

The uncertainty in the integrated luminosity is 2.6% [40]. The uncertainty in the modeling of PU in simulation is assigned by varying the inelastic cross section by $\pm5\%$ [41].

Uncertainties in the differences between efficiencies in data and simulation for the trigger, muon isolation, and muon identification criteria are generally less than 3%.

An uncertainty due to the finite number of simulated events used to construct the response matrix is estimated by randomly varying the content of each bin of the response matrix according to a Poisson uncertainty. The standard deviation of the unfolded results is taken as an estimate of the uncertainty. It ranges from 0.1% to 6.9% for jet multiplicities of 1 to 7.

The effect of the systematic uncertainties on the measured cross section as a function of jet multiplicity is illustrated in Fig. 2. The total uncertainty is the sum in quadrature of all contributions.

9 Results

The measured W($\to \mu\nu$)+jets fiducial cross sections are shown in Figs. 3–15 and compared to the predictions of the LO MC generator MADGRAPH5+PYTHIA6 (described in Section 3),
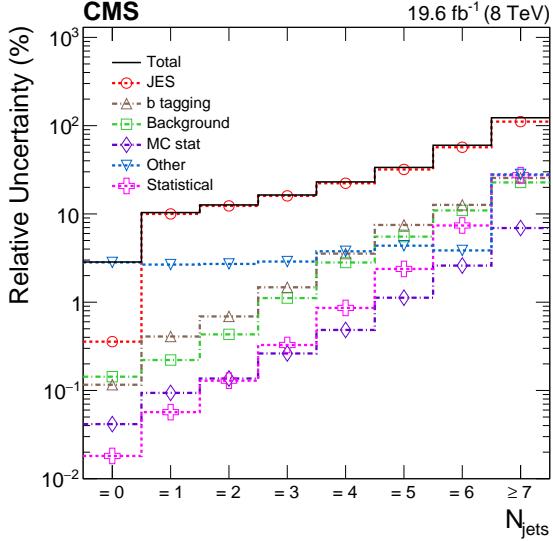
Figure 2: Systematic uncertainties in the measured cross section as a function of jet multiplicity, including uncertainties due to jet energy scale (JES), background normalization, b tagging efficiency, finite number of simulated events used to construct the response matrix (MC stat), and other systematic uncertainties mentioned in Section 8. Statistical uncertainty of the unfolded data and total uncertainty in the measured cross section are also shown.

to those of MADGRAPH5_aMC@NLO and SHERPA NLO MC generators, and to the fixed-order theoretical predictions provided by BLACKHAT+SHERPA [42] and by a W+1 jet NNLO calculation [6, 7]. The 8 TeV data sample allows us to determine the cross sections for jet multiplicities up to 7 and to study the fiducial cross sections as functions of most kinematic observables for up to four jets.

An NLO prediction is provided by MADGRAPH5_aMC@NLO version 2.2.1 [3], a generator with up to three final-state partons, with ME computation for up to two jets at NLO accuracy, which uses the NNPDF3.0 PDF set [43]. The generator is interfaced with PYTHIA 8 [44] for parton showering and hadronization, and the corresponding sample is denoted MAD-GRAPH5_aMC@NLO+PYTHIA8 (denoted as MG5_aMC+PY8 in the figure legends). The merging of parton shower and ME is done with the FxFx merging scheme [45] and the merging scale is set at 30 GeV. The NNPDF2.3 PDF set [46] and the CUETP8M1 tune [47] are used in PYTHIA8. Using the weighting methods available in the generator [48], PDF and scale uncertainties are assigned to the MADGRAPH5_aMC@NLO+PYTHIA8 predictions by considering the NNPDF3.0 PDF uncertainties, and by independently varying the factorization and renormalization scales by a factor of 0.5 or 2, excluding the combinations where one scale is varied by a factor of 0.5 and the other one by a factor of 2.

Another NLO prediction is provided by SHERPA version 2.1.1, a multileg NLO event generator with parton showering interfaced with BLACKHAT [49, 50] for the one-loop corrections. This sample of events is produced with the CT10 PDF set. The corresponding sample is denoted SHERPA 2. The SHERPA 2 matrix element calculations include the production of up to four parton jets, with NLO accuracy for up to two jets and LO accuracy for three and four jets. The merging of parton showers and MEs is done with the MEPS@NLO method [4, 51] and the merging scale set at 20 GeV. The predictions from MADGRAPH5+PYTHIA6 and SHERPA 2 are shown with statistical uncertainties only.

The BLACKHAT+SHERPA samples yield fixed-order NLO predictions for 8 TeV W + n jets at the

level of ME partons, where $n = 1$–4. The choice of renormalization and factorization scales for BLACKHAT+SHERPA is $\hat{H}_T'/2$, where $\hat{H}_T' = \sum_m p_T^m + E_T^W$, the sum running over final-state partons, and E_T^W being the transverse energy of the W boson. A nonperturbative correction is applied to the BLACKHAT+SHERPA distributions to account for the effects of multiple-parton interactions and hadronization. This correction is determined with MADGRAPH 5.1.1 interfaced with PYTHIA 6.426 with and without hadronization and multiple-parton interactions. The nonperturbative correction factor is mostly in the range 0.90–1.20. A PDF uncertainty is assigned to the predictions of BLACKHAT+SHERPA by considering the error sets of CT10 PDFs. A factorization and renormalization scale uncertainty is also assigned to BLACKHAT+SHERPA predictions, as determined by varying the scales simultaneously by a factor of 0.5 or 2.

An NNLO calculation of W+jet production in perturbative QCD is also used for comparisons with the certain measured distributions (leading jet p_T, H_T, and $|\eta|$, Figs. 4, 5, and 8) for $N_{jets} \geq 1$. The CT14 NNLO PDF set is used in the calculation. A nonperturbative correction is applied to this prediction, as in the case of BLACKHAT+SHERPA, as well as an additional correction factor of about 1.01 due to the effect of final-state radiation from the muon. A factorization and renormalization scale uncertainty is assigned to this prediction, as determined by varying the central scale $\sqrt{m_{\ell\nu}^2 + (\sum_{jet} p_T^{jet})^2}$ by a factor of 0.5 or 2.

The measured exclusive and inclusive jet multiplicity distributions, shown in Fig. 3, are in agreement with the predictions of the MADGRAPH5_aMC@NLO+PYTHIA8 generators and with the calculation of BLACKHAT+SHERPA. For multiplicities above 5, SHERPA 2 starts to deviate upward from the measurement.

The cross sections differential in jet p_T for inclusive jet multiplicities from 1 to 4 are shown in Fig. 4. The jet p_T and H_T distributions are sensitive to the effects of higher-order processes. The current results extend to 1.0 and 1.5 TeV in the leading-jet p_T and H_T distributions, respectively, for at least one jet. The predictions from BLACKHAT+SHERPA (jets 1 through 4) are in agreement with the measured distributions within the systematic uncertainties. The predictions from MADGRAPH5+PYTHIA6 show reasonable agreement with data, with the largest discrepancy being an overestimate of up to 20% for the leading and second-leading jet p_T distributions in the intermediate-p_T region. In comparison to the corresponding measurements of the leading and second-leading jet p_T spectra made by CMS with 7 TeV data [12], we observe a smaller slope in the ratio of the MADGRAPH5+PYTHIA6 prediction to the measurement. The predictions from MADGRAPH5_aMC@NLO+PYTHIA8 are in agreement with data within uncertainties. The NNLO prediction for at least one jet agrees with the unfolded jet p_T cross section within the systematic uncertainties. At low p_T values (below 50 GeV), the predictions for the first-, second-, and third-leading jet p_T from SHERPA 2 overestimate the data.

The H_T distributions for inclusive jet multiplicities of 1 to 4 are shown in Fig. 5. The H_T distributions are best modeled by the NNLO prediction for an inclusive jet multiplicity of 1, and by MADGRAPH5+PYTHIA6 and MADGRAPH5_aMC@NLO+PYTHIA8 for inclusive jet multiplicities of 1 and 2. For higher jet multiplicities, the MADGRAPH5+PYTHIA6 and MADGRAPH5_aMC@NLO-+PYTHIA8 predictions underestimate the data at low values of H_T (below 200 GeV). The SHERPA 2 predictions for H_T consistently overestimate the data for all inclusive jet multiplicities and display a harder H_T spectrum. The BLACKHAT+SHERPA prediction underestimates the data H_T distribution for $N_{jets} \geq 1$, as expected because the NLO prediction for H_T for $N_{jets} \geq 1$ is a fixed-order prediction with up to two real partons, and contributions from higher jet multiplicities are missing [52].

The dijet p_T and invariant mass spectra for inclusive jet multiplicities of 2, 3, and 4 are shown in Figs. 6 and 7. Dijet quantities are based on the two leading jets in the event, and they consti-
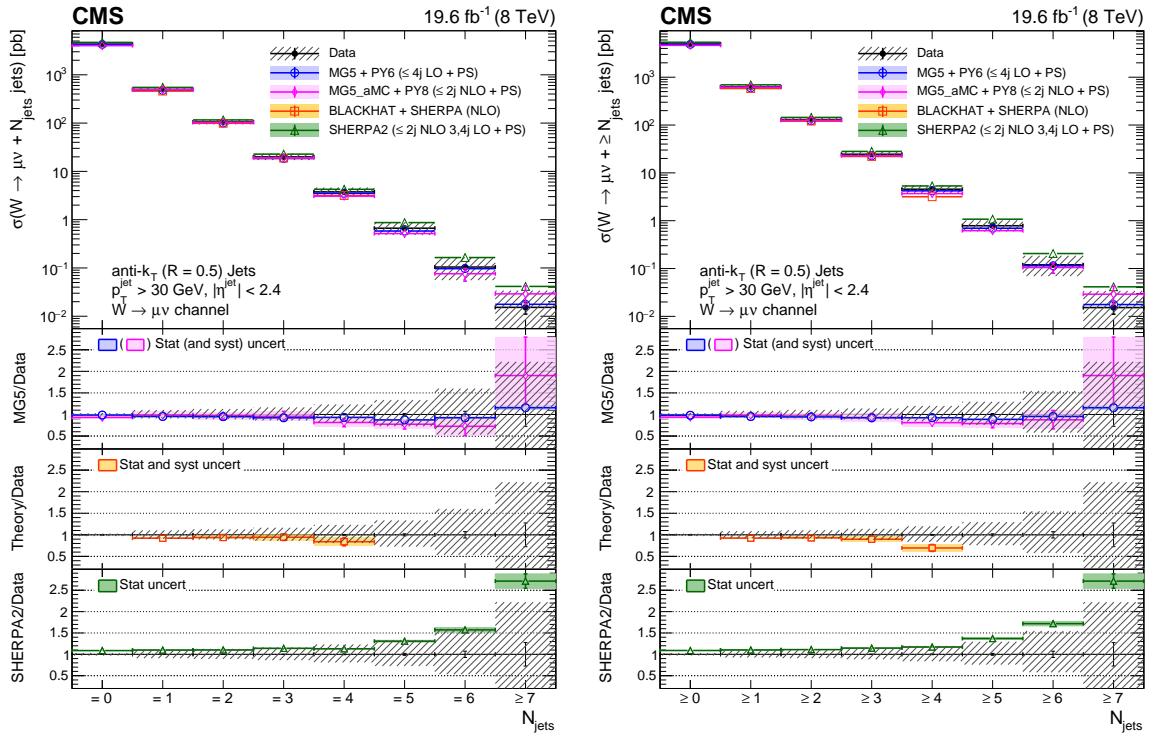
Figure 3: Measured cross section versus exclusive (left) and inclusive (right) jet multiplicity, compared to the predictions of MADGRAPH, MADGRAPH5_aMC@NLO, SHERPA 2, and BLACK-HAT+SHERPA (corrected for hadronization and multiple-parton interactions), for which we currently have predictions only up to $W + 4$ jets. Black circular markers with the gray hatched band represent the unfolded data measurement and its total uncertainty. Overlaid are the predictions together with their uncertainties. The lower plots show the ratio of each prediction to the unfolded data.
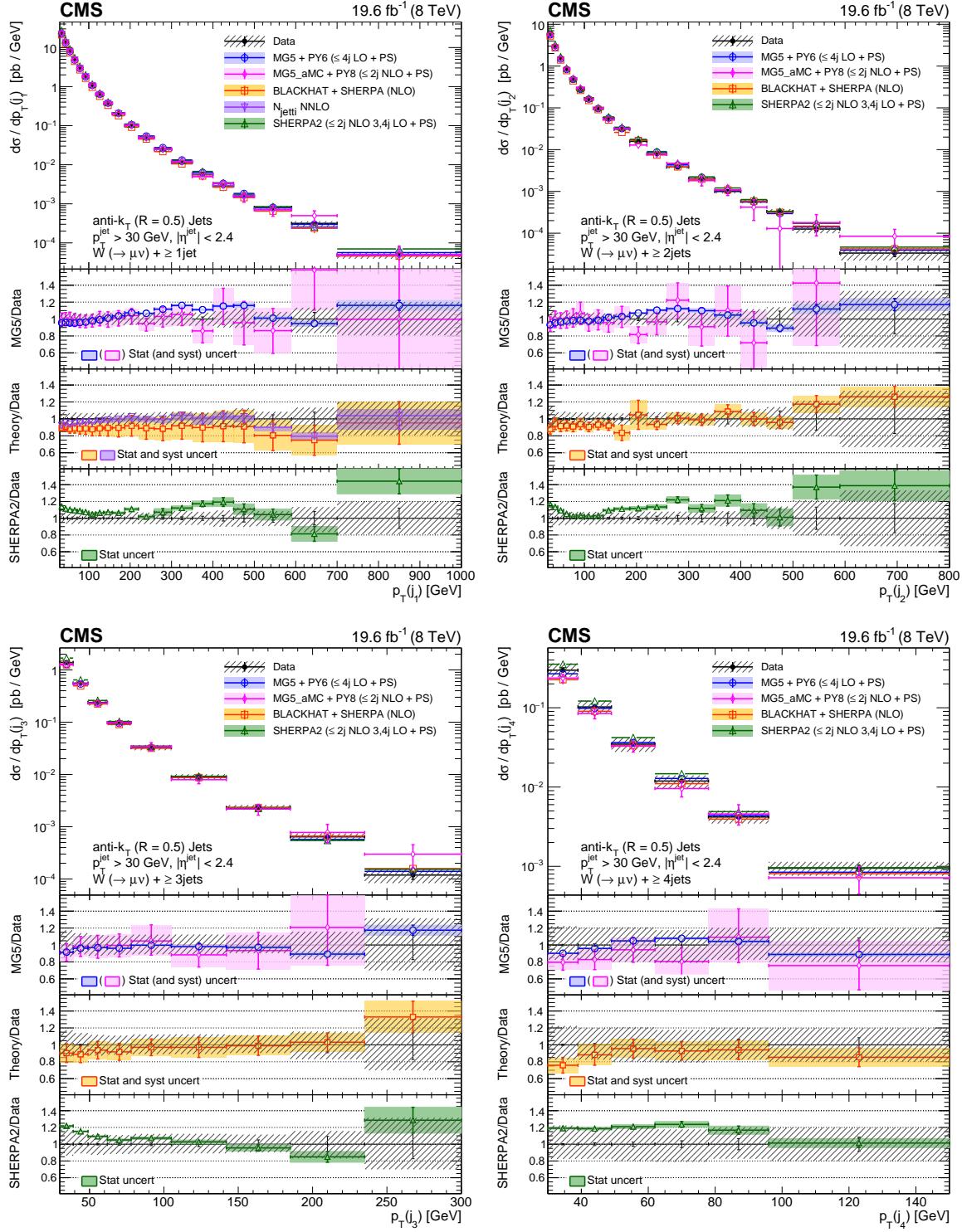
Figure 4: Cross sections differential in the transverse momenta of the four leading jets, compared to the predictions of MADGRAPH, MADGRAPH5_aMC@NLO, SHERPA 2, BLACK-HAT+SHERPA, and NNLO inclusive one-jet production (indicated as N_{jetti} NNLO). The BLACK-HAT+SHERPA and NNLO predictions are corrected for hadronization and multiple-parton interaction effects. Black circular markers with the gray hatched band represent the unfolded data measurements and their total uncertainties. Overlaid are the predictions together with their uncertainties. The lower plots show the ratio of each prediction to the unfolded data.
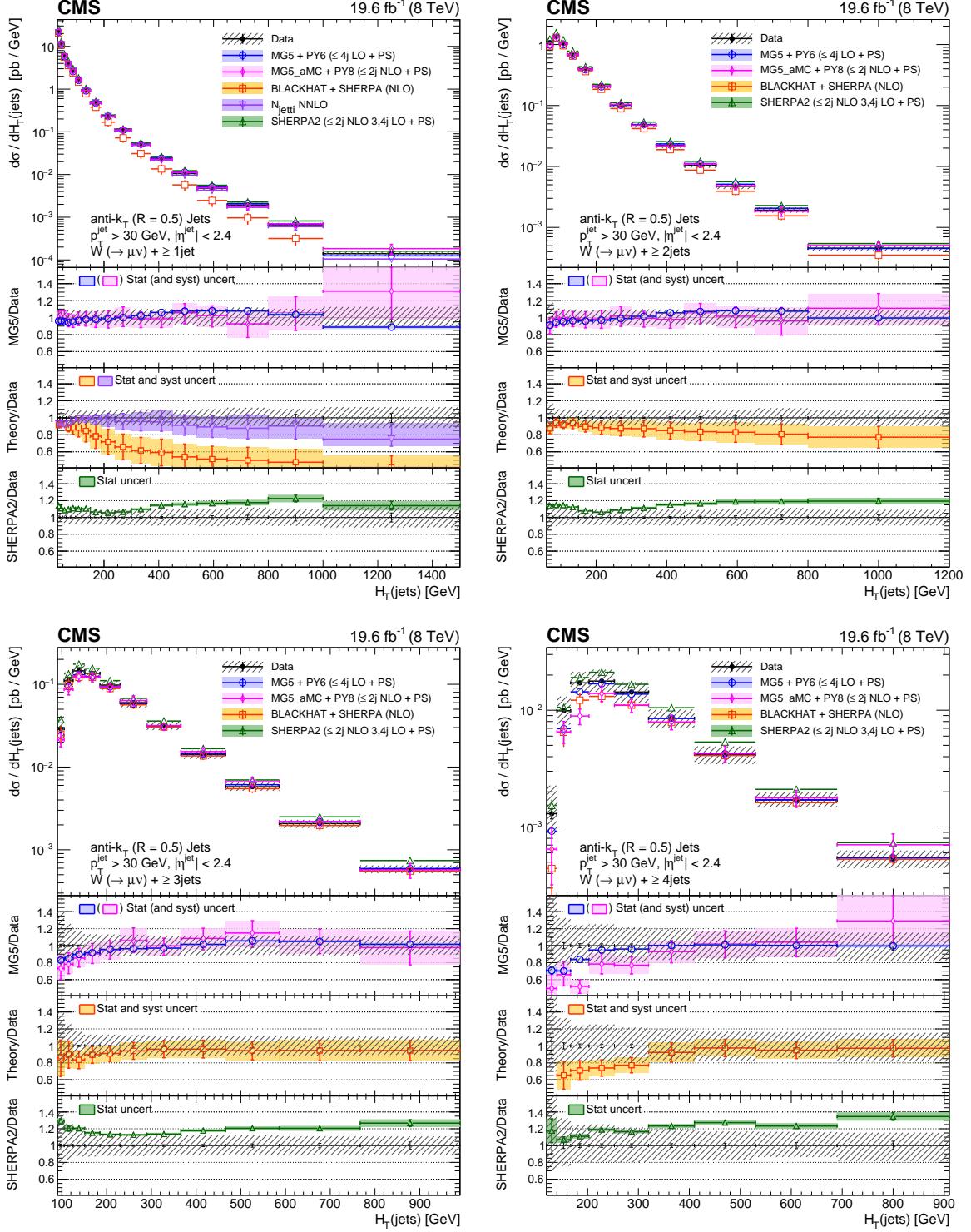
Figure 5: Cross sections differential in H_T for inclusive jet multiplicities 1–4, compared to the predictions of MADGRAPH, MADGRAPH5_aMC@NLO, SHERPA 2, BLACKHAT+SHERPA, and NNLO inclusive one-jet production (indicated as N_{jetti} NNLO). The BLACKHAT+SHERPA and NNLO predictions are corrected for hadronization and multiple-parton interaction effects. Black circular markers with the gray hatched band represent the unfolded data measurements and their total uncertainties. Overlaid are the predictions together with their uncertainties. The lower plots show the ratio of each prediction to the unfolded data.

tute an important test of the modeling of p_T correlations among jets, whose correct accounting is crucial for searches for physics beyond the SM in dijet final states. All of the predictions agree reasonably well with data, but SHERPA 2 consistently overestimates the data for high values of dijet p_T and invariant mass, particularly in the dijet p_T spectrum for $N_{jets} \geq 2$. The MADGRAPH5_aMC@NLO+PYTHIA8 prediction also underestimates the data for values of the invariant mass below 200 GeV in the inclusive four-jet distribution.

The dependence of the cross section on several angular variables and angular correlations between jets is also studied. The pseudorapidity distributions for the four leading jets in each event are shown in Fig. 8. The cross sections are best predicted by MADGRAPH5+PYTHIA6 and MADGRAPH5_aMC@NLO +PYTHIA8. All predictions agree with the data, with some variations in the overall normalization and a slight underestimation for large values of $|\eta|$.

The distributions of the rapidity difference and the azimuthal angles between p_T-ordered and rapidity-ordered jets are shown in Figs. 9–12. The measurement of the rapidity difference between p_T-ordered jets is shown for different jet pairings: the two leading jets $\Delta y(j_1, j_2)$ and the first- (second-) and third-leading jets $\Delta y(j_1, j_3)$ $(\Delta y(j_2, j_3))$. The measurement of the rapidity difference between rapidity-ordered jets makes use of the most forward and most backward jets, $\Delta y(j_F, j_B)$. The quantities $\Delta y(j_1, j_2)$ and $\Delta y(j_F, j_B)$ are studied for inclusive jet multiplicities of 2 to 4, while $\Delta y(j_1, j_3)$ and $\Delta y(j_2, j_3)$ are studied for $N_{jets} \geq 3$. A study of the rapidity difference between the two leading jets is helpful in testing the wide-angle soft parton radiation and the implementation of parton showering. The measurement of the rapidity differences between the forward/backward jets is also instrumental in understanding QCD radiation and wide-angle particle emission. The distribution of the azimuthal angle difference is sensitive to higher-order processes and is shown for p_T-ordered and rapidity-ordered jets for an inclusive multiplicity of 2. Overall, the predicted distributions of the rapidity difference between p_T-ordered jets are in agreement with the measurements, with MADGRAPH5+PYTHIA6 and BLACKHAT+SHERPA underestimating the data for $|\Delta y|$ values above 2. A similar observation can be made for the rapidity difference between the most forward and most backward jets. This behavior is also reflected in the $\Delta R(j_1, j_2)$ measurement, shown in Fig. 13. All predictions for the azimuthal angle difference between jets are in agreement with data, with some variations in the overall normalization.

The distributions of the azimuthal angle between the muon and the leading jet, for inclusive jet multiplicities 1 to 4, are shown in Fig. 14. Overall, the predictions are in agreement with the measurements, except for BLACKHAT+SHERPA, which disagrees with the data at low values of the $\Delta \phi$ for an inclusive jet multiplicity of 1.

Finally, the average number of jets, $\langle N_{jets} \rangle$, is shown as a function of H_T, $\Delta y(j_1, j_2)$, and $\Delta y(j_F, j_B)$ in the inclusive two-jet events in Fig. 15. In the high-H_T region, which is particularly sensitive to higher-order processes, the average number of jets plateaus around a value of 3.5. Although MADGRAPH5+PYTHIA6 tends to underestimate $\langle N_{jets} \rangle$ and SHERPA 2 tends to overestimate it, the deviations are not significant and both generators appear to adequately reproduce the data. Good agreement is observed between the data and all predictions for the dependence of $\langle N_{jets} \rangle$ on the p_T-ordered and rapidity-ordered rapidity differences. These measurements provide an important test of the implementation and modeling of wide-angle gluon emission in the MC generators and NLO calculations. Overall, the accuracy of the predictions for $\langle N_{jets} \rangle$ is much better than was found at the Tevatron [10].
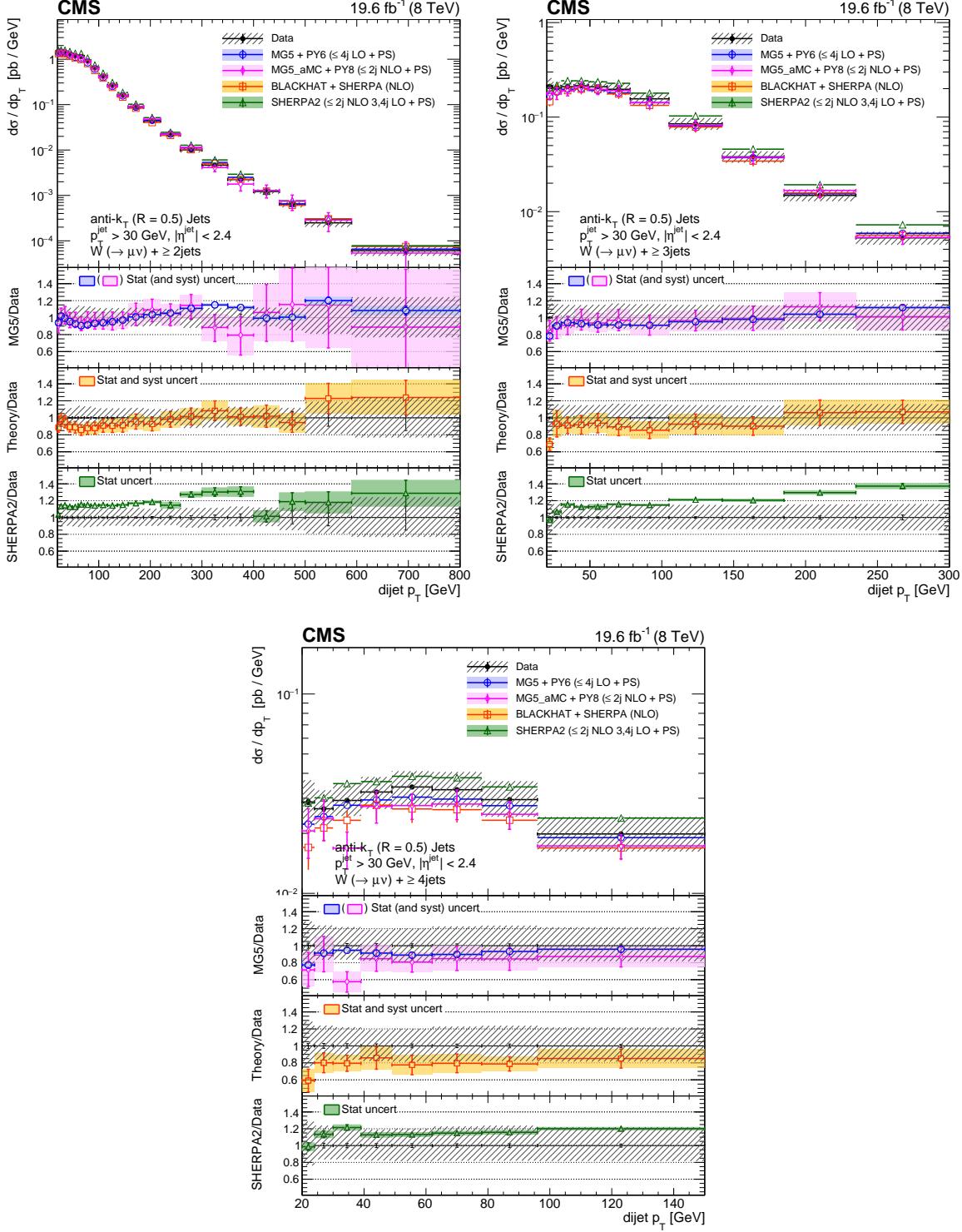
Figure 6: Cross sections differential in dijet p_T (calculated from the two leading jets) for inclusive jet multiplicities 2–4, compared to the predictions of MADGRAPH, MADGRAPH5_aMC@NLO, SHERPA 2, and BLACKHAT+SHERPA (corrected for hadronization and multiple-parton interactions). Black circular markers with the gray hatched band represent the unfolded data measurements and their total uncertainties. Overlaid are the predictions together with their uncertainties. The lower plots show the ratio of each prediction to the unfolded data.
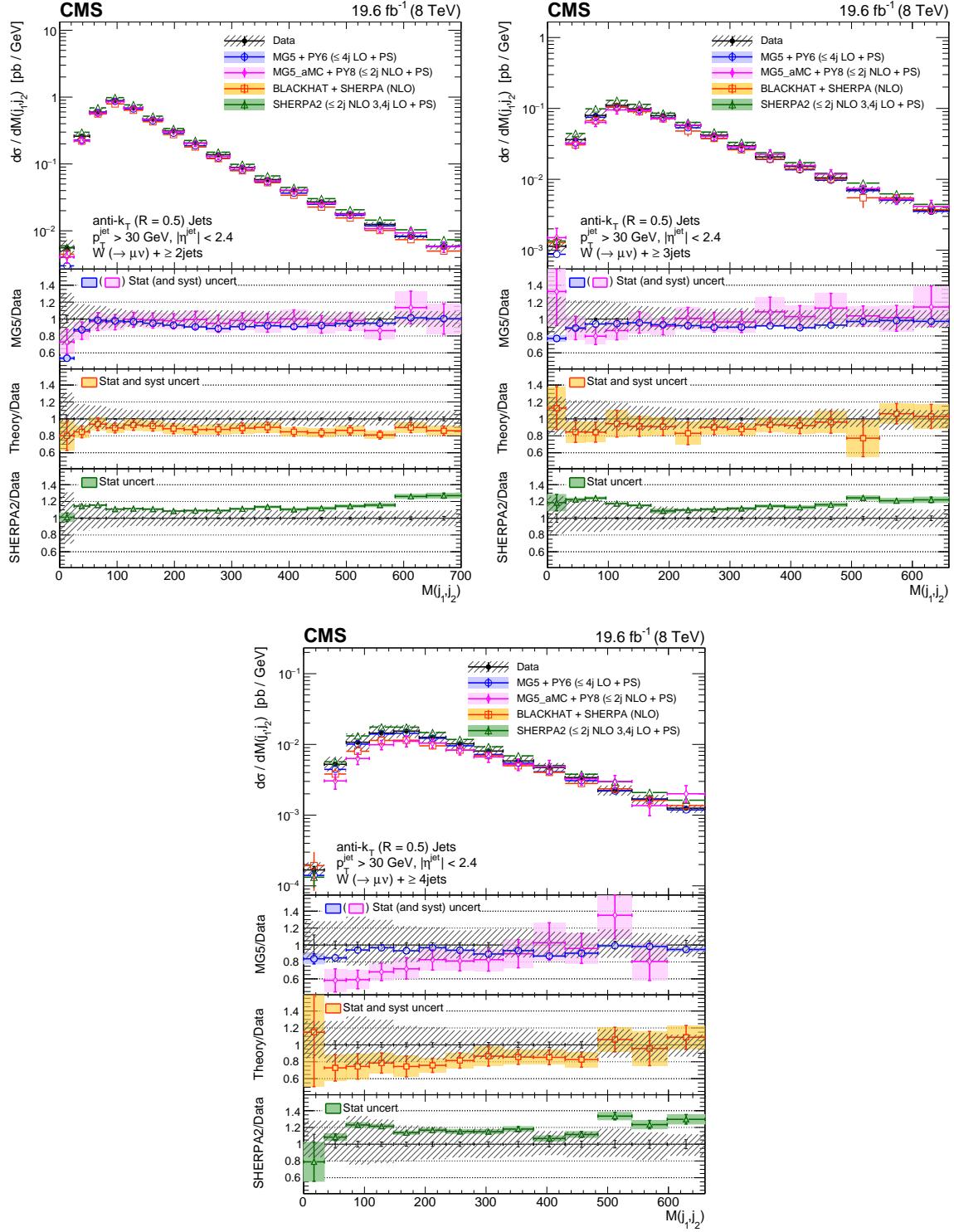
Figure 7: Cross sections differential in dijet invariant mass (calculated from the two leading jets) for inclusive jet multiplicities 2–4, compared to the predictions of MADGRAPH, MAD-GRAPH5_aMC@NLO, SHERPA 2, and BLACKHAT+SHERPA (corrected for hadronization and multiple-parton interactions). Black circular markers with the gray hatched band represent the unfolded data measurements and their total uncertainties. Overlaid are the predictions together with their uncertainties. The lower plots show the ratio of each prediction to the unfolded data.
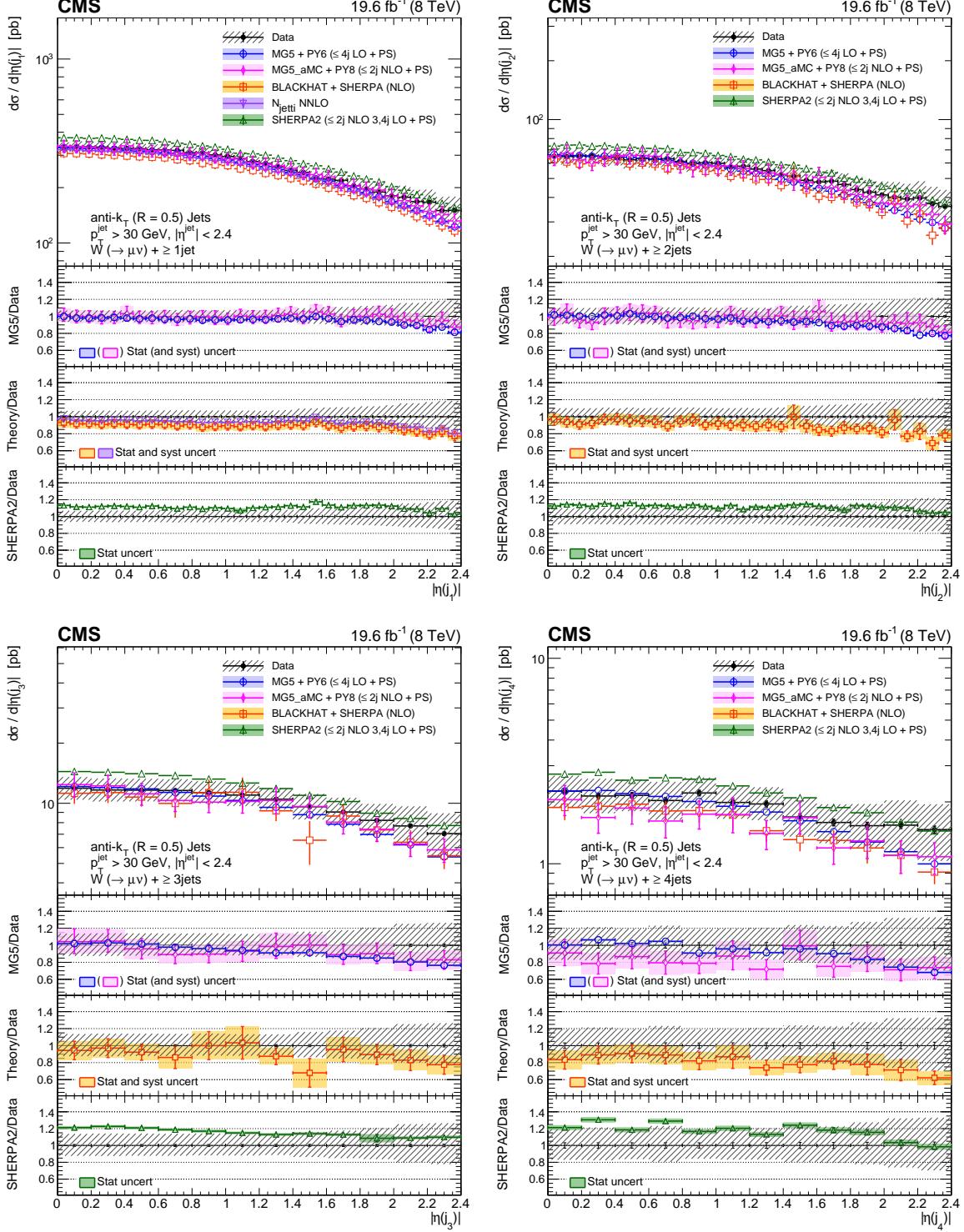
Figure 8: Cross sections differential in the pseudorapidities of the four leading jets, compared to the predictions of MADGRAPH, MADGRAPH5_AMC@NLO, SHERPA 2, BLACKHAT+SHERPA, and NNLO inclusive one-jet production (indicated as N_{jetti} NNLO). The BLACKHAT+SHERPA and NNLO predictions are corrected for hadronization and multiple-parton interaction effects. Black circular markers with the gray hatched band represent the unfolded data measurements and their total uncertainties. Overlaid are the predictions together with their uncertainties. The lower plots show the ratio of each prediction to the unfolded data.
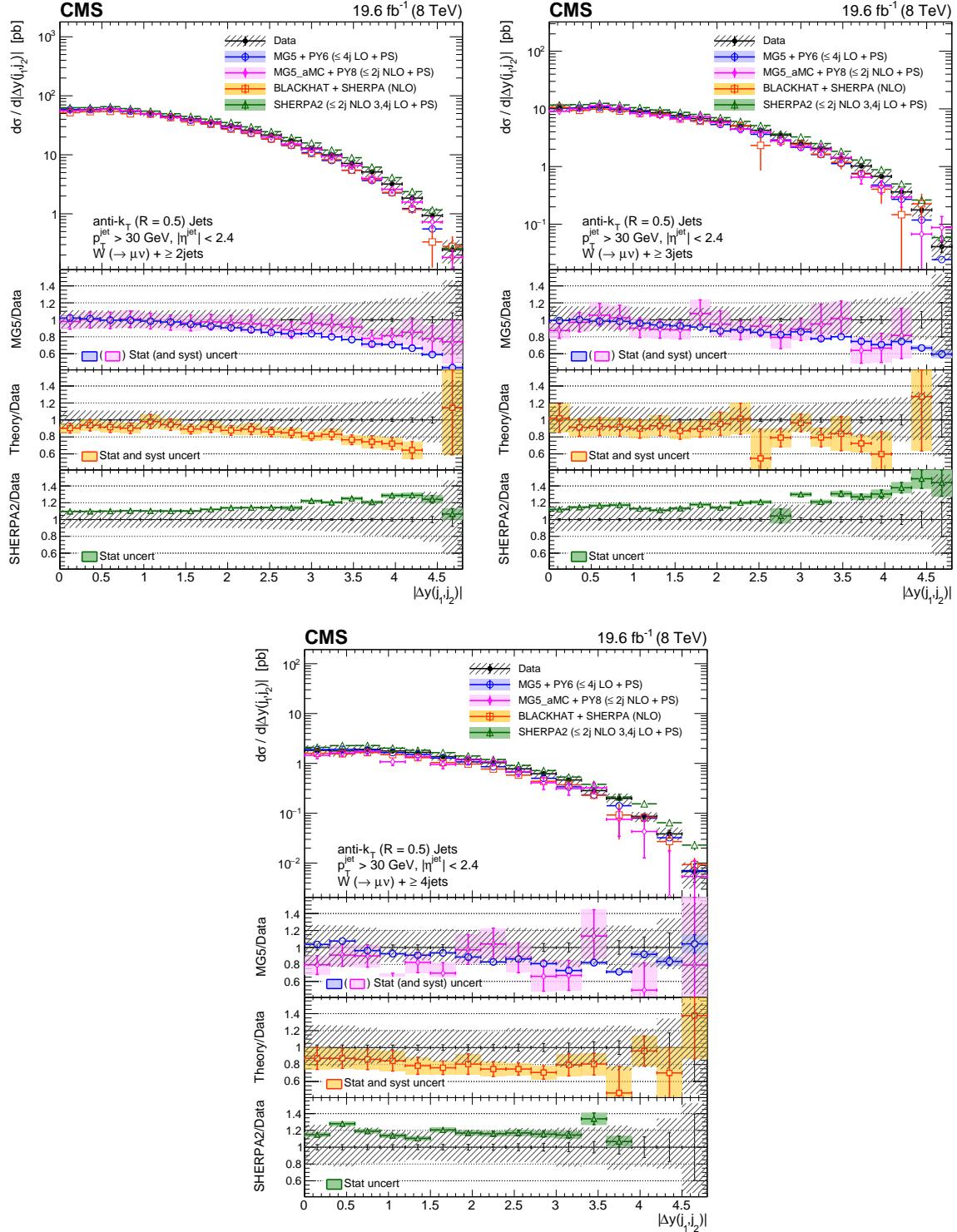
Figure 9: Cross sections differential in $\Delta y(j_1, j_2)$ for inclusive jet multiplicities 2–4, compared to the predictions of MADGRAPH, MADGRAPH5_aMC@NLO, SHERPA 2, and BLACKHAT+SHERPA (corrected for hadronization and multiple-parton interactions). Black circular markers with the gray hatched band represent the unfolded data measurements and their total uncertainties. Overlaid are the predictions together with their uncertainties. The lower plots show the ratio of each prediction to the unfolded data.
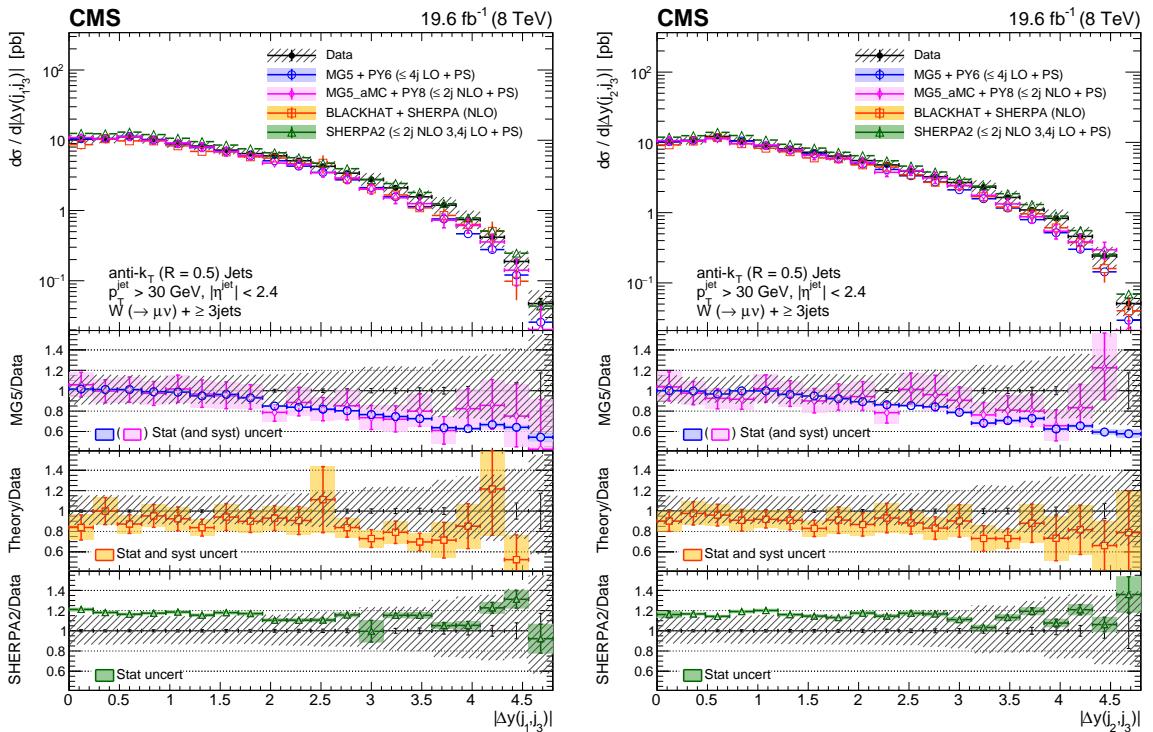
Figure 10: Cross sections differential in $\Delta y(j_1, j_3)$ (left) and $\Delta y(j_2, j_3)$ (right) for an inclusive jet multiplicity of 3, compared to the predictions of MADGRAPH, MADGRAPH5_aMC@NLO, SHERPA 2, and BLACKHAT+SHERPA (corrected for hadronization and multiple-parton interactions). Black circular markers with the gray hatched band represent the unfolded data measurements and their total uncertainties. Overlaid are the predictions together with their uncertainties. The lower plots show the ratio of each prediction to the unfolded data.
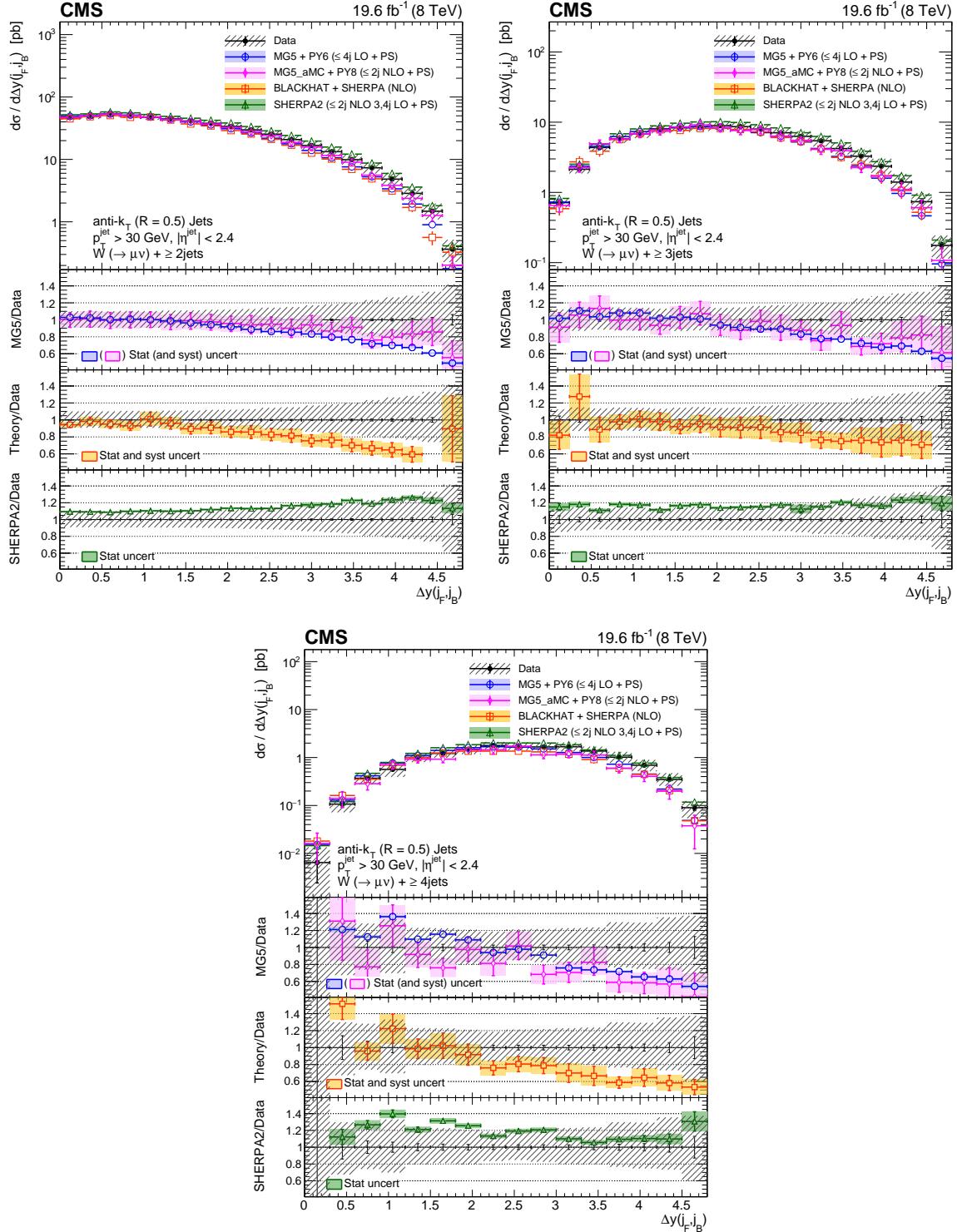
Figure 11: Cross sections differential in $\Delta y(j_F, j_B)$ for inclusive jet multiplicities 2–4, compared to the predictions of MADGRAPH, MADGRAPH5_aMC@NLO, SHERPA 2, and BLACK-HAT+SHERPA (corrected for hadronization and multiple-parton interactions). Black circular markers with the gray hatched band represent the unfolded data measurements and their total uncertainties. Overlaid are the predictions together with their uncertainties. The lower plots show the ratio of each prediction to the unfolded data.
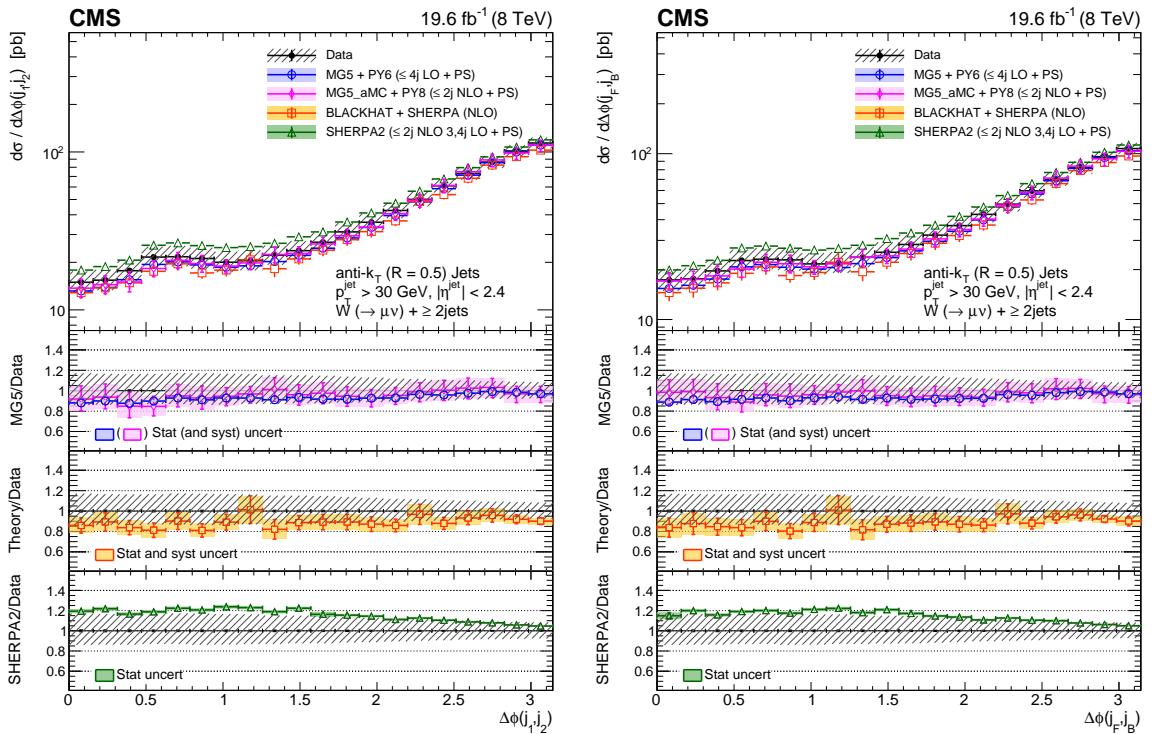
Figure 12: Cross sections differential in $\Delta\phi(j_1, j_2)$ (left) and $\Delta\phi(j_F, j_B)$ (right) for an inclusive jet multiplicity of 2, compared to the predictions of MADGRAPH, MADGRAPH5_aMC@NLO, SHERPA 2, and BLACKHAT+SHERPA (corrected for hadronization and multiple-parton interactions). Black circular markers with the gray hatched band represent the unfolded data measurements and their total uncertainties. Overlaid are the predictions together with their uncertainties. The lower plots show the ratio of each prediction to the unfolded data.
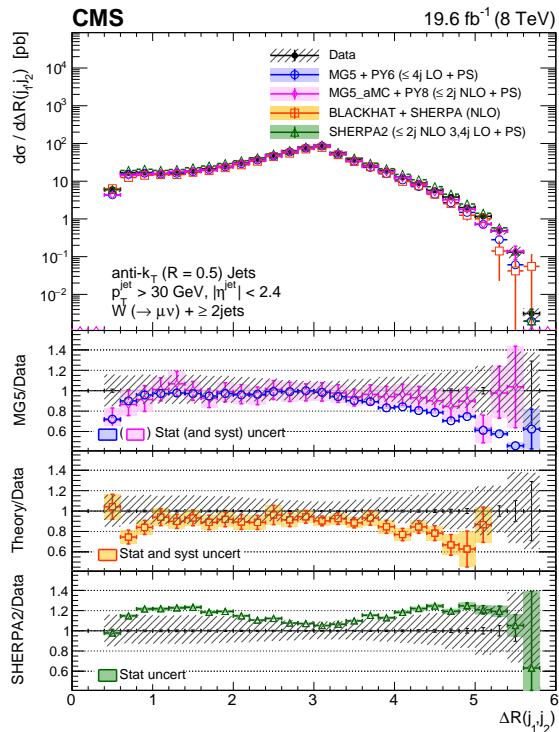
Figure 13: Cross section differential in $\Delta R(j_1, j_2)$ for an inclusive jet multiplicity of 2, compared to the predictions of MADGRAPH, MADGRAPH5_aMC@NLO, SHERPA 2, and BLACK-HAT+SHERPA (corrected for hadronization and multiple-parton interactions). Black circular markers with the gray hatched band represent the unfolded data measurements and their total uncertainties. Overlaid are the predictions together with their uncertainties. The lower plots show the ratio of each prediction to the unfolded data.
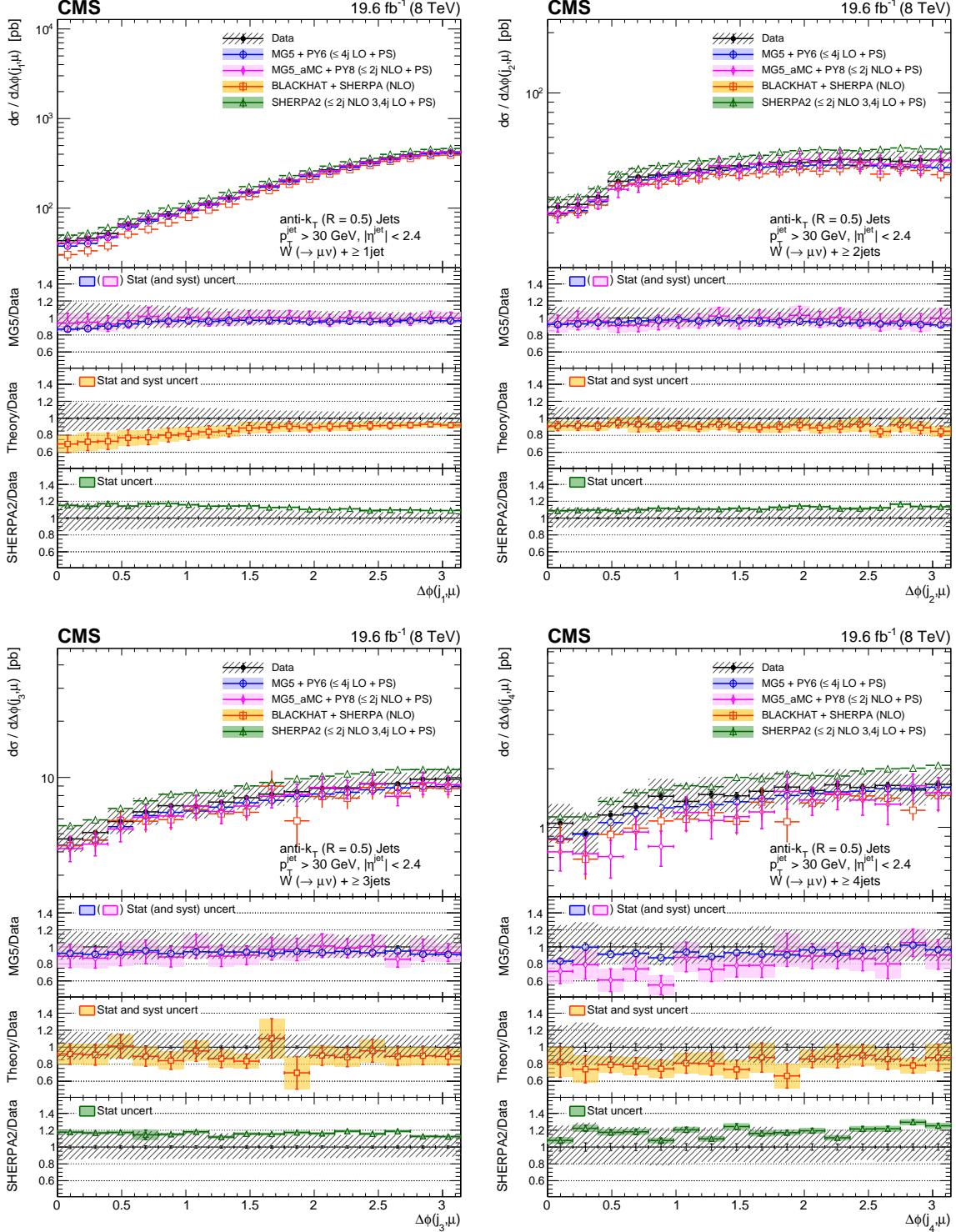
Figure 14: Cross sections differential in $\Delta\phi(j_n, \mu)$ for inclusive jet multiplicities $n = 1$–4, compared to the predictions of MADGRAPH, MADGRAPH5_aMC@NLO, SHERPA 2, and BLACK-HAT+SHERPA (corrected for hadronization and multiple-parton interactions). Black circular markers with the gray hatched band represent the unfolded data measurements and their total uncertainties. Overlaid are the predictions together with their uncertainties. The lower plots show the ratio of each prediction to the unfolded data.
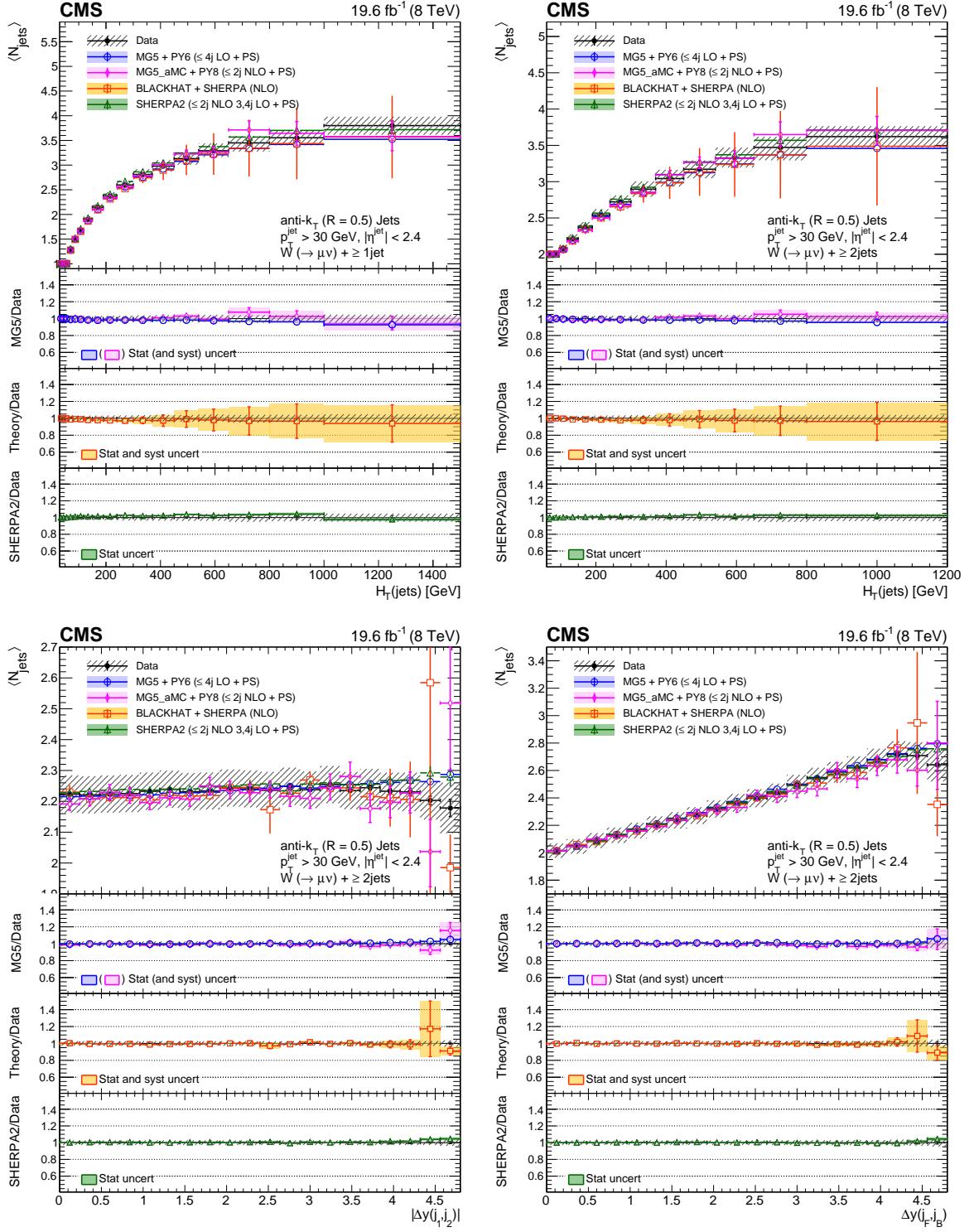
Figure 15: Average number of jets $\langle N_{\text{jets}} \rangle$ as a function of H_T for inclusive jet multiplicities 1–2 (top row) and as a function of $\Delta y(j_1, j_2)$ and $\Delta y(j_F, j_B)$ for an inclusive jet multiplicity of 2 (bottom row), compared to the predictions of MADGRAPH, SHERPA 2, and BLACKHAT+SHERPA (corrected for hadronization and multiple-parton interactions). Black circular markers with the gray hatched band represent the unfolded data measurements and their total uncertainties. Overlaid are the predictions together with their uncertainties. The lower plots show the ratio of each prediction to the unfolded data.

10 Summary

Differential cross sections for a W boson produced in association with jets in pp collisions at a center-of-mass energy of 8 TeV were measured. The data correspond to an integrated luminosity of $19.6\,\text{fb}^{-1}$ and were collected with the CMS detector at the LHC.

Cross sections measured using the muonic decay mode of the W boson were presented as functions of the jet multiplicity, the transverse momenta and pseudorapidities of the four leading jets, H_T for jet multiplicities up to four, and the dijet p_T and invariant mass. Cross sections were also presented as functions of several angular correlation variables: rapidity difference, azimuthal angle difference, and ΔR between p_T-ordered and rapidity-ordered jets, and azimuthal angle difference between the muon and the leading jet. The dependence of the average number of jets on H_T and on rapidity differences between jets was examined.

The results were corrected for detector effects by means of regularized unfolding and compared with particle-level simulated predictions using MADGRAPH5+PYTHIA6; SHERPA 2 and MADGRAPH5_aMC@NLO+PYTHIA8 (multileg NLO); BLACKHAT+SHERPA (NLO); and N_jetti NNLO.

The predictions generally describe the jet multiplicity within the uncertainties, with increasing deviations observed in SHERPA 2 for jet multiplicities greater than 4. The cross sections differential in the p_T of the three leading jets are overestimated by MADGRAPH5+PYTHIA6 in a region of intermediate p_T, and by SHERPA 2 at low p_T. The cross sections as functions of jet p_T predicted by BLACKHAT+SHERPA and by MADGRAPH5_aMC@NLO+PYTHIA8 agree with the measurements within uncertainties.

The cross section as a function of H_T is underestimated by BLACKHAT+SHERPA for $N_\text{jets} \geq 1$ because the contribution from W + $\geq$3 jets is missing from an NLO prediction of W + $\geq$1 jet. The corresponding predictions from SHERPA 2 overestimate the cross section, particularly at high H_T.

The predictions for the jet $|\eta|$ distribution deviate from the measurements for large values of $|\eta|$, as do the predictions for the angular correlation distributions in rapidity for large rapidity differences. Improvement in describing the data at high rapidity difference and at low azimuthal angle difference between muon and jet is observed when considering MADGRAPH5_aMC@NLO+PYTHIA8 versus tree-level MADGRAPH5+PYTHIA6. The distribution of the azimuthal angle between the muon and the leading jet is not well modeled by BLACKHAT+SHERPA for $N_\text{jets} \geq 1$. The predictions for the correlation distributions in azimuthal angle between jets agree with the measurements, as well as the dependence of the average number of jets on angular correlation variables and on H_T.

The NNLO predictions for W+1 jet production were compared with the measured cross sections differential in leading jet p_T, H_T, and leading jet $|\eta|$ and agree with data within uncertainties.

Acknowledgments

References

[1] J. Alwall et al., "MadGraph 5: going beyond", *JHEP* **06** (2011) 128, `doi:10.1007/JHEP06(2011)128`, `arXiv:1106.0522`.

[2] T. Sjöstrand, S. Mrenna, and P. Skands, "PYTHIA 6.4 physics and manual", *JHEP* **05** (2006) 026, `doi:10.1088/1126-6708/2006/05/026`, `arXiv:hep-ph/0603175`.

[3] J. Alwall et al., "The automated computation of tree-level and next-to-leading order differential cross sections, and their matching to parton shower simulations", *JHEP* **07** (2014) 079, `doi:10.1007/JHEP07(2014)079`, `arXiv:1405.0301`.

[4] S. Höche, F. Krauss, M. Schönherr, and F. Siegert, "QCD matrix elements + parton showers: The NLO case", *JHEP* **04** (2013) 027, `doi:10.1007/JHEP04(2013)027`, `arXiv:1207.5030`.

[5] Z. Bern et al., "Ntuples for NLO events at hadron colliders", *Comput. Phys. Commun.* **185** (2014) 1443, `doi:10.1016/j.cpc.2014.01.011`, `arXiv:1310.7439`.

[6] R. Boughezal, C. Focke, X. Liu, and F. Petriello, "W-boson production in association with a jet at next-to-next-to-leading order in perturbative QCD", *Phys. Rev. Lett.* **115** (2015) 062002, `doi:10.1103/PhysRevLett.115.062002`, `arXiv:1504.02131`.

[7] R. Boughezal, X. Liu, and F. Petriello, "W-boson plus jet differential distributions at NNLO in QCD", (2016). `arXiv:1602.06965`.

[8] CDF Collaboration, "Measurement of the cross section for W-boson production in association with jets in p$\overline{\mathrm{p}}$ collisions at $\sqrt{s} = 1.96$ TeV", *Phys. Rev. D* **77** (2008) 011108, `doi:10.1103/PhysRevD.77.011108`, `arXiv:0711.4044`.

[9] D0 Collaboration, "Measurements of inclusive W+jets production rates as a function of jet transverse momentum in p$\overline{\mathrm{p}}$ collisions at $\sqrt{s} = 1.96$ TeV", *Phys. Lett. B* **705** (2011) 200, `doi:10.1016/j.physletb.2011.10.011`, `arXiv:1106.1457`.

[10] D0 Collaboration, "Studies of W boson plus jets production in $p\bar{p}$ collisions at $\sqrt{s} = 1.96$ TeV", *Phys. Rev. D* **88** (2013) 092001, `doi:10.1103/PhysRevD.88.092001`, `arXiv:1302.6508`.

[11] ATLAS Collaboration, "Measurements of the W production cross sections in association with jets with the ATLAS detector", *Eur. Phys. J. C* **75** (2015) 82, `doi:10.1140/epjc/s10052-015-3262-7`, `arXiv:1409.8639`.

[12] CMS Collaboration, "Differential cross section measurements for the production of a W boson in association with jets in proton-proton collisions at $\sqrt{s} = 7$ TeV", *Phys. Lett. B* **741** (2015) 12, `doi:10.1016/j.physletb.2014.12.003`, `arXiv:1406.7533`.

[13] CMS Collaboration, "The CMS experiment at the CERN LHC", *JINST* **3** (2008) S08004, `doi:10.1088/1748-0221/3/08/S08004`.

[14] GEANT4 Collaboration, "GEANT4—a simulation toolkit", *Nucl. Instrum. Meth. A* **506** (2003) 250, `doi:10.1016/S0168-9002(03)01368-8`.

[15] CMS Collaboration, "Charged particle multiplicities in pp interactions at $\sqrt{s} = 0.9, 2.36$, and 7 TeV", *JHEP* **01** (2010) 079, `doi:10.1007/JHEP01(2011)079`, `arXiv:1011.5531`.

[16] J. Pumplin et al., "New generation of parton distributions with uncertainties from global QCD analysis", *JHEP* **07** (2002) 012, `doi:10.1088/1126-6708/2002/07/012`, `arXiv:hep-ph/0201195`.

[17] K. Melnikov and F. Petriello, "Electroweak gauge boson production at hadron colliders through $O(\alpha_S^2)$", *Phys. Rev. D* **74** (2006) 114017, `doi:10.1103/PhysRevD.74.114017`, `arXiv:hep-ph/0609070`.

[18] J. Alwall et al., "Comparative study of various algorithms for the merging of parton showers and matrix elements in hadronic collisions", *Eur. Phys. J. C* **53** (2008) 473, `doi:10.1140/epjc/s10052-007-0490-5`, `arXiv:0706.2569`.

[19] M. Cacciari, G. P. Salam, and G. Soyez, "FastJet user manual", *Eur. Phys. J. C* **72** (2012) 1896, `doi:10.1140/epjc/s10052-012-1896-2`, `arXiv:1111.6097`.

[20] P. Nason, "A new method for combining NLO QCD with shower Monte Carlo algorithms", *JHEP* **11** (2004) 040, `doi:10.1088/1126-6708/2004/11/040`, `arXiv:hep-ph/0409146`.

[21] S. Frixione, P. Nason, and C. Oleari, "Matching NLO QCD computations with parton shower simulations: the POWHEG method", *JHEP* **11** (2007) 070, `doi:10.1088/1126-6708/2007/11/070`, `arXiv:0709.2092`.

[22] S. Alioli, P. Nason, C. Oleari, and E. Re, "A general framework for implementing NLO calculations in shower Monte Carlo programs: the POWHEG BOX", *JHEP* **06** (2010) 043, `doi:10.1007/JHEP06(2010)043`, `arXiv:1002.2581`.

[23] S. Alioli, P. Nason, C. Oleari, and E. Re, "NLO single-top production matched with shower in POWHEG: s- and t-channel contributions", *JHEP* **09** (2009) 111, `doi:10.1088/1126-6708/2009/09/111`, `arXiv:0907.4076`.

[24] J. Campbell, R. K. Ellis, and F. Tramontano, "Single top-quark production and decay at next-to-leading order", *Phys. Rev. D* **70** (2004) 094012, `doi:10.1103/PhysRevD.70.094012`, `arXiv:hep-ph/0408158`.

[25] J. Campbell and F. Tramontano, "Next-to-leading order corrections to Wt production and decay", *Nucl. Phys. B* **726** (2005) 109, `doi:10.1016/j.nuclphysb.2005.08.015`, `arXiv:hep-ph/0506289`.

[26] J. M. Campbell, R. Frederix, F. Maltoni, and F. Tramontano, "Next-to-Leading-Order Predictions for t-Channel Single-Top Production at Hadron Colliders", *Phys. Rev. Lett.* **102** (2009) 182003, `doi:10.1103/PhysRevLett.102.182003`, `arXiv:0903.0005`.

[27] J. M. Campbell, R. K. Ellis, and C. Williams, "Vector boson pair production at the LHC", *JHEP* **07** (2011) 018, `doi:10.1007/JHEP07(2011)018`, `arXiv:1105.0020`.

[28] M. Czakon, P. Fiedler, and A. Mitov, "The total top quark pair production cross-section at hadron colliders through $\mathrm{O}(\alpha_S^4)$", *Phys. Rev. Lett.* **110** (2013) 252004, `doi:10.1103/PhysRevLett.110.252004`, `arXiv:1303.6254`.

[29] CMS Collaboration, "Particle–Flow Event Reconstruction in CMS and Performance for Jets, Taus, and E_T^{miss}", CMS Physics Analysis Summary CMS-PAS-PFT-09-001, 2009.

[30] CMS Collaboration, "Commissioning of the particle-flow event reconstruction with the first LHC collisions recorded in the CMS detector", CMS Physics Analysis Summary CMS-PAS-PFT-10-001, 2010.

[31] CMS Collaboration, "Performance of CMS muon reconstruction in pp collision events at $\sqrt{s} = 7\,\mathrm{TeV}$", *JINST* **7** (2012) P10002, `doi:10.1088/1748-0221/7/10/P10002`, `arXiv:1206.4071`.

[32] M. Cacciari, G. P. Salam, and G. Soyez, "The anti-k_T jet clustering algorithm", *JHEP* **04** (2008) 063, `doi:10.1088/1126-6708/2008/04/063`, `arXiv:0802.1189`.

[33] CMS Collaboration, "Determination of jet energy calibration and transverse momentum resolution in CMS", *JINST* **6** (2011) 11002, `doi:10.1088/1748-0221/6/11/P11002`, `arXiv:1107.4277`.

[34] CMS Collaboration, "Identification of b-quark jets with the CMS experiment", *JINST* **8** (2013) 04013, `doi:10.1088/1748-0221/8/04/P04013`, `arXiv:1211.4462`.

[35] G. D'Agostini, "A multidimensional unfolding method based on Bayes theorem", *Nucl. Instr. Meth. A* **362** (1995) 487, `doi:10.1016/0168-9002(95)00274-X`.

[36] T. Adye, "Unfolding algorithms and tests using RooUnfold", in *PHYSTAT 2011 Workshop on Statistical Issues Related to Discovery Claims in Search Experiments and Unfolding*, H. Prosper and L. Lyons, eds., p. 313. CERN, Geneva, Switzerland, 2011. `arXiv:1105.1160`. `doi:10.5170/CERN-2011-006.313`.

[37] A. Höcker and V. Kartvelishvili, "SVD approach to data unfolding", *Nucl. Instrum. Meth. A* **372** (1996) 469, `doi:10.1016/0168-9002(95)01478-0`, `arXiv:hep-ph/9509307`.

[38] J. Campbell and R. K. Ellis, "Next-to-leading order corrections to W+2 jet and Z+2 jet production at hadron colliders", *Phys. Rev. D* **65** (2002) 113007, `doi:10.1103/PhysRevD.65.113007`, `arXiv:hep-ph/0202176`.

[39] CMS Collaboration, "Performance of b tagging at $\sqrt{s} = 8\,\mathrm{TeV}$ in multijet, $t\bar{t}$, and boosted topology events", CMS Physics Analysis Summary CMS-PAS-BTV-13-001, 2013.

[40] CMS Collaboration, "CMS Luminosity Based on Pixel Cluster Counting - Summer 2013 Update", CMS Physics Analysis Summary CMS-PAS-LUM-13-001, 2013.

[41] CMS Collaboration, "Measurement of the inelastic proton-proton cross section at $\sqrt{s} = 7\,\mathrm{TeV}$", *Phys. Lett. B* **722** (2013) 5, `doi:10.1016/j.physletb.2013.03.024`, `arXiv:1210.6718`.

[42] C. F. Berger et al., "Next-to-leading order QCD predictions for W+3-jet distributions at hadron colliders", *Phys. Rev. D* **80** (2009) 074036, `doi:10.1103/PhysRevD.80.074036`, `arXiv:0907.1984`.

[43] NNPDF Collaboration, "Parton distributions for the LHC Run II", *JHEP* **04** (2015) 040, `doi:10.1007/JHEP04(2015)040`, `arXiv:1410.8849`.

[44] T. Sjöstrand, S. Mrenna, and P. Z. Skands, "A brief introduction to PYTHIA 8.1", *Comput. Phys. Commun.* **178** (2007) 852, `doi:10.1016/j.cpc.2008.01.036`, `arXiv:0710.3820`.

[45] R. Frederix and S. Frixione, "Merging meets matching in MC@NLO", *JHEP* **12** (2012) 061, `doi:10.1007/JHEP12(2012)061`, `arXiv:1209.6215`.

[46] NNPDF Collaboration, M. Ubiali, "Towards the NNPDF3.0 parton set for the next LHC run", in *Proceedings of the XXII Int'l Workshop on Deep-Inelastic Scattering and Related Subjects*, volume 07, p. 041. Warsaw, Poland, May, 2014. `arXiv:1407.3122`. PoS(DIS2014)041.

[47] CMS Collaboration, "Event generator tunes obtained from underlying event and multiparton scattering measurements", *Eur. Phys. J. C* **76** (2016) 155, `doi:10.1140/epjc/s10052-016-3988-x`, `arXiv:1512.00815`.

[48] R. Frederix et al., "Four-lepton production at hadron colliders: aMC@NLO predictions with theoretical uncertainties", *JHEP* **02** (2012) 099, `doi:10.1007/JHEP02(2012)099`, `arXiv:1110.4738`.

[49] C. F. Berger et al., "One-Loop Calculations with BlackHat", in *Proceedings of the 9th DESY Workshop on Elementary Particle Theory*. 2008. `arXiv:0807.3705`. Nucl. Phys. Proc. Suppl. 183 (2008) 313. `doi:10.1016/j.nuclphysbps.2008.09.123`.

[50] C. F. Berger et al., "Vector Boson + Jets with BlackHat and SHERPA", in *Loops and Legs in Quantum Field Theory — Proccedings of the 10th DESY Workshop on Elementary Particle Theory*. 2010. `arXiv:1005.3728`. Nucl. Phys. Proc. Suppl. 205-206 (2010) 92. `doi:10.1016/j.nuclphysbps.2010.08.025`.

[51] S. Hoeche, F. Krauss, M. Schonherr, and F. Siegert, "A critical appraisal of NLO+PS matching methods", *JHEP* **09** (2012) 049, `doi:10.1007/JHEP09(2012)049`, `arXiv:1111.1220`.

[52] D. Maître and S. Sapeta, "Simulated NNLO for high-p_T observables in vector boson + jets production at the LHC", *Eur. Phys. J. C* **73** (2013) 2663, `doi:10.1140/epjc/s10052-013-2663-8`, `arXiv:1307.2252`.

A   The CMS Collaboration

Yerevan Physics Institute, Yerevan, Armenia
V. Khachatryan, A.M. Sirunyan, A. Tumasyan

Institut für Hochenergiephysik, Wien, Austria
W. Adam, E. Asilar, T. Bergauer, J. Brandstetter, E. Brondolin, M. Dragicevic, J. Erö, M. Flechl, M. Friedl, R. Frühwirth[1], V.M. Ghete, C. Hartl, N. Hörmann, J. Hrubec, M. Jeitler[1], A. König, I. Krätschmer, D. Liko, T. Matsushita, I. Mikulec, D. Rabady, N. Rad, B. Rahbaran, H. Rohringer, J. Schieck[1], J. Strauss, W. Treberer-Treberspurg, W. Waltenberger, C.-E. Wulz[1]

National Centre for Particle and High Energy Physics, Minsk, Belarus
V. Mossolov, N. Shumeiko, J. Suarez Gonzalez

Universiteit Antwerpen, Antwerpen, Belgium
S. Alderweireldt, E.A. De Wolf, X. Janssen, J. Lauwers, M. Van De Klundert, H. Van Haevermaet, P. Van Mechelen, N. Van Remortel, A. Van Spilbeeck

Vrije Universiteit Brussel, Brussel, Belgium
S. Abu Zeid, F. Blekman, J. D'Hondt, N. Daci, I. De Bruyn, K. Deroover, N. Heracleous, S. Lowette, S. Moortgat, L. Moreels, A. Olbrechts, Q. Python, S. Tavernier, W. Van Doninck, P. Van Mulders, I. Van Parijs

Université Libre de Bruxelles, Bruxelles, Belgium
H. Brun, C. Caillol, B. Clerbaux, G. De Lentdecker, H. Delannoy, G. Fasanella, L. Favart, R. Goldouzian, A. Grebenyuk, G. Karapostoli, T. Lenzi, A. Léonard, J. Luetic, T. Maerschalk, A. Marinov, A. Randle-conde, T. Seva, C. Vander Velde, P. Vanlaer, R. Yonamine, F. Zenoni, F. Zhang[2]

Ghent University, Ghent, Belgium
A. Cimmino, T. Cornelis, D. Dobur, A. Fagot, G. Garcia, M. Gul, D. Poyraz, S. Salva, R. Schöfbeck, M. Tytgat, W. Van Driessche, E. Yazgan, N. Zaganidis

Université Catholique de Louvain, Louvain-la-Neuve, Belgium
H. Bakhshiansohi, C. Beluffi[3], O. Bondu, S. Brochet, G. Bruno, A. Caudron, S. De Visscher, C. Delaere, M. Delcourt, B. Francois, A. Giammanco, A. Jafari, P. Jez, M. Komm, V. Lemaitre, A. Magitteri, A. Mertens, M. Musich, C. Nuttens, K. Piotrzkowski, L. Quertenmont, M. Selvaggi, M. Vidal Marono, S. Wertz

Université de Mons, Mons, Belgium
N. Beliy

Centro Brasileiro de Pesquisas Fisicas, Rio de Janeiro, Brazil
W.L. Aldá Júnior, F.L. Alves, G.A. Alves, L. Brito, C. Hensel, A. Moraes, M.E. Pol, P. Rebello Teles

Universidade do Estado do Rio de Janeiro, Rio de Janeiro, Brazil
E. Belchior Batista Das Chagas, W. Carvalho, J. Chinellato[4], A. Custódio, E.M. Da Costa, G.G. Da Silveira[5], D. De Jesus Damiao, C. De Oliveira Martins, S. Fonseca De Souza, L.M. Huertas Guativa, H. Malbouisson, D. Matos Figueiredo, C. Mora Herrera, L. Mundim, H. Nogima, W.L. Prado Da Silva, A. Santoro, A. Sznajder, E.J. Tonelli Manganote[4], A. Vilela Pereira

Universidade Estadual Paulista [a], Universidade Federal do ABC [b], São Paulo, Brazil
S. Ahuja[a], C.A. Bernardes[b], S. Dogra[a], T.R. Fernandez Perez Tomei[a], E.M. Gregores[b],

P.G. Mercadante[b], C.S. Moon[a], S.F. Novaes[a], Sandra S. Padula[a], D. Romero Abad[b], J.C. Ruiz Vargas

Institute for Nuclear Research and Nuclear Energy, Sofia, Bulgaria
A. Aleksandrov, R. Hadjiiska, P. Iaydjiev, M. Rodozov, S. Stoykova, G. Sultanov, M. Vutova

University of Sofia, Sofia, Bulgaria
A. Dimitrov, I. Glushkov, L. Litov, B. Pavlov, P. Petkov

Beihang University, Beijing, China
W. Fang[6]

Institute of High Energy Physics, Beijing, China
M. Ahmad, J.G. Bian, G.M. Chen, H.S. Chen, M. Chen, Y. Chen[7], T. Cheng, C.H. Jiang, D. Leggat, Z. Liu, F. Romeo, S.M. Shaheen, A. Spiezia, J. Tao, C. Wang, Z. Wang, H. Zhang, J. Zhao

State Key Laboratory of Nuclear Physics and Technology, Peking University, Beijing, China
Y. Ban, G. Chen, Q. Li, S. Liu, Y. Mao, S.J. Qian, D. Wang, Z. Xu

Universidad de Los Andes, Bogota, Colombia
C. Avila, A. Cabrera, L.F. Chaparro Sierra, C. Florez, J.P. Gomez, C.F. González Hernández, J.D. Ruiz Alvarez, J.C. Sanabria

University of Split, Faculty of Electrical Engineering, Mechanical Engineering and Naval Architecture, Split, Croatia
N. Godinovic, D. Lelas, I. Puljak, P.M. Ribeiro Cipriano, T. Sculac

University of Split, Faculty of Science, Split, Croatia
Z. Antunovic, M. Kovac

Institute Rudjer Boskovic, Zagreb, Croatia
V. Brigljevic, D. Ferencek, K. Kadija, S. Micanovic, L. Sudic, T. Susa

University of Cyprus, Nicosia, Cyprus
A. Attikis, G. Mavromanolakis, J. Mousa, C. Nicolaou, F. Ptochos, P.A. Razis, H. Rykaczewski

Charles University, Prague, Czech Republic
M. Finger[8], M. Finger Jr.[8]

Universidad San Francisco de Quito, Quito, Ecuador
E. Carrera Jarrin

Academy of Scientific Research and Technology of the Arab Republic of Egypt, Egyptian Network of High Energy Physics, Cairo, Egypt
A.A. Abdelalim[9,10], Y. Mohammed[11], E. Salama[12,13]

National Institute of Chemical Physics and Biophysics, Tallinn, Estonia
B. Calpas, M. Kadastik, M. Murumaa, L. Perrini, M. Raidal, A. Tiko, C. Veelken

Department of Physics, University of Helsinki, Helsinki, Finland
P. Eerola, J. Pekkanen, M. Voutilainen

Helsinki Institute of Physics, Helsinki, Finland
J. Härkönen, V. Karimäki, R. Kinnunen, T. Lampén, K. Lassila-Perini, S. Lehti, T. Lindén, P. Luukka, T. Peltola, J. Tuominiemi, E. Tuovinen, L. Wendland

Lappeenranta University of Technology, Lappeenranta, Finland
J. Talvitie, T. Tuuva

IRFU, CEA, Université Paris-Saclay, Gif-sur-Yvette, France
M. Besancon, F. Couderc, M. Dejardin, D. Denegri, B. Fabbro, J.L. Faure, C. Favaro, F. Ferri, S. Ganjour, S. Ghosh, A. Givernaud, P. Gras, G. Hamel de Monchenault, P. Jarry, I. Kucher, E. Locci, M. Machet, J. Malcles, J. Rander, A. Rosowsky, M. Titov, A. Zghiche

Laboratoire Leprince-Ringuet, Ecole Polytechnique, IN2P3-CNRS, Palaiseau, France
A. Abdulsalam, I. Antropov, S. Baffioni, F. Beaudette, P. Busson, L. Cadamuro, E. Chapon, C. Charlot, O. Davignon, R. Granier de Cassagnac, M. Jo, S. Lisniak, P. Miné, M. Nguyen, C. Ochando, G. Ortona, P. Paganini, P. Pigard, S. Regnard, R. Salerno, Y. Sirois, T. Strebler, Y. Yilmaz, A. Zabi

Institut Pluridisciplinaire Hubert Curien, Université de Strasbourg, Université de Haute Alsace Mulhouse, CNRS/IN2P3, Strasbourg, France
J.-L. Agram[14], J. Andrea, A. Aubin, D. Bloch, J.-M. Brom, M. Buttignol, E.C. Chabert, N. Chanon, C. Collard, E. Conte[14], X. Coubez, J.-C. Fontaine[14], D. Gelé, U. Goerlach, A.-C. Le Bihan, K. Skovpen, P. Van Hove

Centre de Calcul de l'Institut National de Physique Nucleaire et de Physique des Particules, CNRS/IN2P3, Villeurbanne, France
S. Gadrat

Université de Lyon, Université Claude Bernard Lyon 1, CNRS-IN2P3, Institut de Physique Nucléaire de Lyon, Villeurbanne, France
S. Beauceron, C. Bernet, G. Boudoul, E. Bouvier, C.A. Carrillo Montoya, R. Chierici, D. Contardo, B. Courbon, P. Depasse, H. El Mamouni, J. Fan, J. Fay, S. Gascon, M. Gouzevitch, G. Grenier, B. Ille, F. Lagarde, I.B. Laktineh, M. Lethuillier, L. Mirabito, A.L. Pequegnot, S. Perries, A. Popov[15], D. Sabes, V. Sordini, M. Vander Donckt, P. Verdier, S. Viret

Georgian Technical University, Tbilisi, Georgia
A. Khvedelidze[8]

Tbilisi State University, Tbilisi, Georgia
Z. Tsamalaidze[8]

RWTH Aachen University, I. Physikalisches Institut, Aachen, Germany
C. Autermann, S. Beranek, L. Feld, A. Heister, M.K. Kiesel, K. Klein, M. Lipinski, A. Ostapchuk, M. Preuten, F. Raupach, S. Schael, C. Schomakers, J.F. Schulte, J. Schulz, T. Verlage, H. Weber, V. Zhukov[15]

RWTH Aachen University, III. Physikalisches Institut A, Aachen, Germany
M. Brodski, E. Dietz-Laursonn, D. Duchardt, M. Endres, M. Erdmann, S. Erdweg, T. Esch, R. Fischer, A. Güth, M. Hamer, T. Hebbeker, C. Heidemann, K. Hoepfner, S. Knutzen, M. Merschmeyer, A. Meyer, P. Millet, S. Mukherjee, M. Olschewski, K. Padeken, T. Pook, M. Radziej, H. Reithler, M. Rieger, F. Scheuch, L. Sonnenschein, D. Teyssier, S. Thüer

RWTH Aachen University, III. Physikalisches Institut B, Aachen, Germany
V. Cherepanov, G. Flügge, W. Haj Ahmad, F. Hoehle, B. Kargoll, T. Kress, A. Künsken, J. Lingemann, T. Müller, A. Nehrkorn, A. Nowack, I.M. Nugent, C. Pistone, O. Pooth, A. Stahl[16]

Deutsches Elektronen-Synchrotron, Hamburg, Germany
M. Aldaya Martin, C. Asawatangtrakuldee, K. Beernaert, O. Behnke, U. Behrens, A.A. Bin Anuar, K. Borras[17], A. Campbell, P. Connor, C. Contreras-Campana, F. Costanza, C. Diez

Pardos, G. Dolinska, G. Eckerlin, D. Eckstein, E. Eren, E. Gallo[18], J. Garay Garcia, A. Geiser, A. Gizhko, J.M. Grados Luyando, P. Gunnellini, A. Harb, J. Hauk, M. Hempel[19], H. Jung, A. Kalogeropoulos, O. Karacheban[19], M. Kasemann, J. Keaveney, J. Kieseler, C. Kleinwort, I. Korol, D. Krücker, W. Lange, A. Lelek, J. Leonard, K. Lipka, A. Lobanov, W. Lohmann[19], R. Mankel, I.-A. Melzer-Pellmann, A.B. Meyer, G. Mittag, J. Mnich, A. Mussgiller, E. Ntomari, D. Pitzl, R. Placakyte, A. Raspereza, B. Roland, M.Ö. Sahin, P. Saxena, T. Schoerner-Sadenius, C. Seitz, S. Spannagel, N. Stefaniuk, K.D. Trippkewitz, G.P. Van Onsem, R. Walsh, C. Wissing

University of Hamburg, Hamburg, Germany
V. Blobel, M. Centis Vignali, A.R. Draeger, T. Dreyer, E. Garutti, D. Gonzalez, J. Haller, M. Hoffmann, A. Junkes, R. Klanner, R. Kogler, N. Kovalchuk, T. Lapsien, T. Lenz, I. Marchesini, D. Marconi, M. Meyer, M. Niedziela, D. Nowatschin, F. Pantaleo[16], T. Peiffer, A. Perieanu, J. Poehlsen, C. Sander, C. Scharf, P. Schleper, A. Schmidt, S. Schumann, J. Schwandt, H. Stadie, G. Steinbrück, F.M. Stober, M. Stöver, H. Tholen, D. Troendle, E. Usai, L. Vanelderen, A. Vanhoefer, B. Vormwald

Institut für Experimentelle Kernphysik, Karlsruhe, Germany
C. Barth, C. Baus, J. Berger, E. Butz, T. Chwalek, F. Colombo, W. De Boer, A. Dierlamm, S. Fink, R. Friese, M. Giffels, A. Gilbert, P. Goldenzweig, D. Haitz, F. Hartmann[16], S.M. Heindl, U. Husemann, I. Katkov[15], P. Lobelle Pardo, B. Maier, H. Mildner, M.U. Mozer, Th. Müller, M. Plagge, G. Quast, K. Rabbertz, S. Röcker, F. Roscher, M. Schröder, I. Shvetsov, G. Sieber, H.J. Simonis, R. Ulrich, J. Wagner-Kuhr, S. Wayand, M. Weber, T. Weiler, S. Williamson, C. Wöhrmann, R. Wolf

Institute of Nuclear and Particle Physics (INPP), NCSR Demokritos, Aghia Paraskevi, Greece
G. Anagnostou, G. Daskalakis, T. Geralis, V.A. Giakoumopoulou, A. Kyriakis, D. Loukas, I. Topsis-Giotis

National and Kapodistrian University of Athens, Athens, Greece
S. Kesisoglou, A. Panagiotou, N. Saoulidou, E. Tziaferi

University of Ioánnina, Ioánnina, Greece
I. Evangelou, G. Flouris, C. Foudas, P. Kokkas, N. Loukas, N. Manthos, I. Papadopoulos, E. Paradas

MTA-ELTE Lendület CMS Particle and Nuclear Physics Group, Eötvös Loránd University, Budapest, Hungary
N. Filipovic

Wigner Research Centre for Physics, Budapest, Hungary
G. Bencze, C. Hajdu, P. Hidas, D. Horvath[20], F. Sikler, V. Veszpremi, G. Vesztergombi[21], A.J. Zsigmond

Institute of Nuclear Research ATOMKI, Debrecen, Hungary
N. Beni, S. Czellar, J. Karancsi[22], A. Makovec, J. Molnar, Z. Szillasi

University of Debrecen, Debrecen, Hungary
M. Bartók[21], P. Raics, Z.L. Trocsanyi, B. Ujvari

National Institute of Science Education and Research, Bhubaneswar, India
S. Bahinipati, S. Choudhury[23], P. Mal, K. Mandal, A. Nayak[24], D.K. Sahoo, N. Sahoo, S.K. Swain

Panjab University, Chandigarh, India
S. Bansal, S.B. Beri, V. Bhatnagar, R. Chawla, U.Bhawandeep, A.K. Kalsi, A. Kaur, M. Kaur, R. Kumar, A. Mehta, M. Mittal, J.B. Singh, G. Walia

University of Delhi, Delhi, India
Ashok Kumar, A. Bhardwaj, B.C. Choudhary, R.B. Garg, S. Keshri, S. Malhotra, M. Naimuddin, N. Nishu, K. Ranjan, R. Sharma, V. Sharma

Saha Institute of Nuclear Physics, Kolkata, India
R. Bhattacharya, S. Bhattacharya, K. Chatterjee, S. Dey, S. Dutt, S. Dutta, S. Ghosh, N. Majumdar, A. Modak, K. Mondal, S. Mukhopadhyay, S. Nandan, A. Purohit, A. Roy, D. Roy, S. Roy Chowdhury, S. Sarkar, M. Sharan, S. Thakur

Indian Institute of Technology Madras, Madras, India
P.K. Behera

Bhabha Atomic Research Centre, Mumbai, India
R. Chudasama, D. Dutta, V. Jha, V. Kumar, A.K. Mohanty[16], P.K. Netrakanti, L.M. Pant, P. Shukla, A. Topkar

Tata Institute of Fundamental Research-A, Mumbai, India
T. Aziz, S. Dugad, G. Kole, B. Mahakud, S. Mitra, G.B. Mohanty, B. Parida, N. Sur, B. Sutar

Tata Institute of Fundamental Research-B, Mumbai, India
S. Banerjee, S. Bhowmik[25], R.K. Dewanjee, S. Ganguly, M. Guchait, Sa. Jain, S. Kumar, M. Maity[25], G. Majumder, K. Mazumdar, T. Sarkar[25], N. Wickramage[26]

Indian Institute of Science Education and Research (IISER), Pune, India
S. Chauhan, S. Dube, V. Hegde, A. Kapoor, K. Kothekar, A. Rane, S. Sharma

Institute for Research in Fundamental Sciences (IPM), Tehran, Iran
H. Behnamian, S. Chenarani[27], E. Eskandari Tadavani, S.M. Etesami[27], A. Fahim[28], M. Khakzad, M. Mohammadi Najafabadi, M. Naseri, S. Paktinat Mehdiabadi[29], F. Rezaei Hosseinabadi, B. Safarzadeh[30], M. Zeinali

University College Dublin, Dublin, Ireland
M. Felcini, M. Grunewald

INFN Sezione di Bari [a], Università di Bari [b], Politecnico di Bari [c], Bari, Italy
M. Abbrescia[a,b], C. Calabria[a,b], C. Caputo[a,b], A. Colaleo[a], D. Creanza[a,c], L. Cristella[a,b], N. De Filippis[a,c], M. De Palma[a,b], L. Fiore[a], G. Iaselli[a,c], G. Maggi[a,c], M. Maggi[a], G. Miniello[a,b], S. My[a,b], S. Nuzzo[a,b], A. Pompili[a,b], G. Pugliese[a,c], R. Radogna[a,b], A. Ranieri[a], G. Selvaggi[a,b], L. Silvestris[a,16], R. Venditti[a,b], P. Verwilligen[a]

INFN Sezione di Bologna [a], Università di Bologna [b], Bologna, Italy
G. Abbiendi[a], C. Battilana, D. Bonacorsi[a,b], S. Braibant-Giacomelli[a,b], L. Brigliadori[a,b], R. Campanini[a,b], P. Capiluppi[a,b], A. Castro[a,b], F.R. Cavallo[a], S.S. Chhibra[a,b], G. Codispoti[a,b], M. Cuffiani[a,b], G.M. Dallavalle[a], F. Fabbri[a], A. Fanfani[a,b], D. Fasanella[a,b], P. Giacomelli[a], C. Grandi[a], L. Guiducci[a,b], S. Marcellini[a], G. Masetti[a], A. Montanari[a], F.L. Navarria[a,b], A. Perrotta[a], A.M. Rossi[a,b], T. Rovelli[a,b], G.P. Siroli[a,b], N. Tosi[a,b,16]

INFN Sezione di Catania [a], Università di Catania [b], Catania, Italy
S. Albergo[a,b], M. Chiorboli[a,b], S. Costa[a,b], A. Di Mattia[a], F. Giordano[a,b], R. Potenza[a,b], A. Tricomi[a,b], C. Tuve[a,b]

INFN Sezione di Firenze ^{a}, Università di Firenze ^{b}, Firenze, Italy
G. Barbagli^a, V. Ciulli^{a,b}, C. Civinini^a, R. D'Alessandro^{a,b}, E. Focardi^{a,b}, V. Gori^{a,b}, P. Lenzi^{a,b}, M. Meschini^a, S. Paoletti^a, G. Sguazzoni^a, L. Viliani^{a,b,16}

INFN Laboratori Nazionali di Frascati, Frascati, Italy
L. Benussi, S. Bianco, F. Fabbri, D. Piccolo, F. Primavera^{16}

INFN Sezione di Genova ^{a}, Università di Genova ^{b}, Genova, Italy
V. Calvelli^{a,b}, F. Ferro^a, M. Lo Vetere^{a,b}, M.R. Monge^{a,b}, E. Robutti^a, S. Tosi^{a,b}

INFN Sezione di Milano-Bicocca ^{a}, Università di Milano-Bicocca ^{b}, Milano, Italy
L. Brianza^{16}, M.E. Dinardo^{a,b}, S. Fiorendi^{a,b}, S. Gennai^a, A. Ghezzi^{a,b}, P. Govoni^{a,b}, M. Malberti, S. Malvezzi^a, R.A. Manzoni^{a,b,16}, B. Marzocchi^{a,b}, D. Menasce^a, L. Moroni^a, M. Paganoni^{a,b}, D. Pedrini^a, S. Pigazzini, S. Ragazzi^{a,b}, T. Tabarelli de Fatis^{a,b}

INFN Sezione di Napoli ^{a}, Università di Napoli 'Federico II' ^{b}, Napoli, Italy, Università della Basilicata ^{c}, Potenza, Italy, Università G. Marconi ^{d}, Roma, Italy
S. Buontempo^a, N. Cavallo^{a,c}, G. De Nardo, S. Di Guida^{a,d,16}, M. Esposito^{a,b}, F. Fabozzi^{a,c}, A.O.M. Iorio^{a,b}, G. Lanza^a, L. Lista^a, S. Meola^{a,d,16}, P. Paolucci^{a,16}, C. Sciacca^{a,b}, F. Thyssen

INFN Sezione di Padova ^{a}, Università di Padova ^{b}, Padova, Italy, Università di Trento ^{c}, Trento, Italy
P. Azzi^{a,16}, M. Bellato^a, L. Benato^{a,b}, D. Bisello^{a,b}, A. Boletti^{a,b}, R. Carlin^{a,b}, A. Carvalho Antunes De Oliveira^{a,b}, P. Checchia^a, M. Dall'Osso^{a,b}, P. De Castro Manzano^a, T. Dorigo^a, U. Dosselli^a, F. Gasparini^{a,b}, U. Gasparini^{a,b}, F. Gonella^a, A. Gozzelino^a, S. Lacaprara^a, M. Margoni^{a,b}, J. Pazzini^{a,b,16}, N. Pozzobon^{a,b}, P. Ronchese^{a,b}, M. Sgaravatto^a, F. Simonetto^{a,b}, E. Torassa^a, P. Zotto^{a,b}, A. Zucchetta^{a,b}, G. Zumerle^{a,b}

INFN Sezione di Pavia ^{a}, Università di Pavia ^{b}, Pavia, Italy
A. Braghieri^a, A. Magnani^{a,b}, P. Montagna^{a,b}, S.P. Ratti^{a,b}, V. Re^a, C. Riccardi^{a,b}, P. Salvini^a, I. Vai^{a,b}, P. Vitulo^{a,b}

INFN Sezione di Perugia ^{a}, Università di Perugia ^{b}, Perugia, Italy
L. Alunni Solestizi^{a,b}, G.M. Bilei^a, D. Ciangottini^{a,b}, L. Fanò^{a,b}, P. Lariccia^{a,b}, R. Leonardi^{a,b}, G. Mantovani^{a,b}, M. Menichelli^a, A. Saha^a, A. Santocchia^{a,b}

INFN Sezione di Pisa ^{a}, Università di Pisa ^{b}, Scuola Normale Superiore di Pisa ^{c}, Pisa, Italy
K. Androsov^{a,31}, P. Azzurri^{a,16}, G. Bagliesi^a, J. Bernardini^a, T. Boccali^a, R. Castaldi^a, M.A. Ciocci^{a,31}, R. Dell'Orso^a, S. Donato^{a,c}, G. Fedi, A. Giassi^a, M.T. Grippo^{a,31}, F. Ligabue^{a,c}, T. Lomtadze^a, L. Martini^{a,b}, A. Messineo^{a,b}, F. Palla^a, A. Rizzi^{a,b}, A. Savoy-Navarro^{a,32}, P. Spagnolo^a, R. Tenchini^a, G. Tonelli^{a,b}, A. Venturi^a, P.G. Verdini^a

INFN Sezione di Roma ^{a}, Università di Roma ^{b}, Roma, Italy
L. Barone^{a,b}, F. Cavallari^a, M. Cipriani^{a,b}, G. D'imperio^{a,b,16}, D. Del Re^{a,b,16}, M. Diemoz^a, S. Gelli^{a,b}, E. Longo^{a,b}, F. Margaroli^{a,b}, P. Meridiani^a, G. Organtini^{a,b}, R. Paramatti^a, F. Preiato^{a,b}, S. Rahatlou^{a,b}, C. Rovelli^a, F. Santanastasio^{a,b}

INFN Sezione di Torino ^{a}, Università di Torino ^{b}, Torino, Italy, Università del Piemonte Orientale ^{c}, Novara, Italy
N. Amapane^{a,b}, R. Arcidiacono^{a,c,16}, S. Argiro^{a,b}, M. Arneodo^{a,c}, N. Bartosik^a, R. Bellan^{a,b}, C. Biino^a, N. Cartiglia^a, F. Cenna^{a,b}, M. Costa^{a,b}, R. Covarelli^{a,b}, A. Degano^{a,b}, N. Demaria^a, L. Finco^{a,b}, B. Kiani^{a,b}, C. Mariotti^a, S. Maselli^a, E. Migliore^{a,b}, V. Monaco^{a,b}, E. Monteil^{a,b}, M.M. Obertino^{a,b}, L. Pacher^{a,b}, N. Pastrone^a, M. Pelliccioni^a, G.L. Pinna Angioni^{a,b}, F. Ravera^{a,b},

A. Romero[a,b], M. Ruspa[a,c], R. Sacchi[a,b], K. Shchelina[a,b], V. Sola[a], A. Solano[a,b], A. Staiano[a], P. Traczyk[a,b]

INFN Sezione di Trieste [a], Università di Trieste [b], Trieste, Italy
S. Belforte[a], M. Casarsa[a], F. Cossutti[a], G. Della Ricca[a,b], C. La Licata[a,b], A. Schizzi[a,b], A. Zanetti[a]

Kyungpook National University, Daegu, Korea
D.H. Kim, G.N. Kim, M.S. Kim, S. Lee, S.W. Lee, Y.D. Oh, S. Sekmen, D.C. Son, Y.C. Yang

Chonbuk National University, Jeonju, Korea
A. Lee

Hanyang University, Seoul, Korea
J.A. Brochero Cifuentes, T.J. Kim

Korea University, Seoul, Korea
S. Cho, S. Choi, Y. Go, D. Gyun, S. Ha, B. Hong, Y. Jo, Y. Kim, B. Lee, K. Lee, K.S. Lee, S. Lee, J. Lim, S.K. Park, Y. Roh

Seoul National University, Seoul, Korea
J. Almond, J. Kim, H. Lee, S.B. Oh, B.C. Radburn-Smith, S.h. Seo, U.K. Yang, H.D. Yoo, G.B. Yu

University of Seoul, Seoul, Korea
M. Choi, H. Kim, H. Kim, J.H. Kim, J.S.H. Lee, I.C. Park, G. Ryu, M.S. Ryu

Sungkyunkwan University, Suwon, Korea
Y. Choi, J. Goh, C. Hwang, J. Lee, I. Yu

Vilnius University, Vilnius, Lithuania
V. Dudenas, A. Juodagalvis, J. Vaitkus

National Centre for Particle Physics, Universiti Malaya, Kuala Lumpur, Malaysia
I. Ahmed, Z.A. Ibrahim, J.R. Komaragiri, M.A.B. Md Ali[33], F. Mohamad Idris[34], W.A.T. Wan Abdullah, M.N. Yusli, Z. Zolkapli

Centro de Investigacion y de Estudios Avanzados del IPN, Mexico City, Mexico
H. Castilla-Valdez, E. De La Cruz-Burelo, I. Heredia-De La Cruz[35], A. Hernandez-Almada, R. Lopez-Fernandez, R. Magaña Villalba, J. Mejia Guisao, A. Sanchez-Hernandez

Universidad Iberoamericana, Mexico City, Mexico
S. Carrillo Moreno, C. Oropeza Barrera, F. Vazquez Valencia

Benemerita Universidad Autonoma de Puebla, Puebla, Mexico
S. Carpinteyro, I. Pedraza, H.A. Salazar Ibarguen, C. Uribe Estrada

Universidad Autónoma de San Luis Potosí, San Luis Potosí, Mexico
A. Morelos Pineda

University of Auckland, Auckland, New Zealand
D. Krofcheck

University of Canterbury, Christchurch, New Zealand
P.H. Butler

National Centre for Physics, Quaid-I-Azam University, Islamabad, Pakistan
A. Ahmad, M. Ahmad, Q. Hassan, H.R. Hoorani, W.A. Khan, M.A. Shah, M. Shoaib, M. Waqas

National Centre for Nuclear Research, Swierk, Poland
H. Bialkowska, M. Bluj, B. Boimska, T. Frueboes, M. Górski, M. Kazana, K. Nawrocki, K. Romanowska-Rybinska, M. Szleper, P. Zalewski

Institute of Experimental Physics, Faculty of Physics, University of Warsaw, Warsaw, Poland
K. Bunkowski, A. Byszuk[36], K. Doroba, A. Kalinowski, M. Konecki, J. Krolikowski, M. Misiura, M. Olszewski, M. Walczak

Laboratório de Instrumentação e Física Experimental de Partículas, Lisboa, Portugal
P. Bargassa, C. Beirão Da Cruz E Silva, A. Di Francesco, P. Faccioli, P.G. Ferreira Parracho, M. Gallinaro, J. Hollar, N. Leonardo, L. Lloret Iglesias, M.V. Nemallapudi, J. Rodrigues Antunes, J. Seixas, O. Toldaiev, D. Vadruccio, J. Varela, P. Vischia

Joint Institute for Nuclear Research, Dubna, Russia
P. Bunin, M. Gavrilenko, I. Golutvin, V. Karjavin, V. Korenkov, A. Lanev, A. Malakhov, V. Matveev[37,38], V.V. Mitsyn, P. Moisenz, V. Palichik, V. Perelygin, S. Shmatov, S. Shulha, N. Skatchkov, V. Smirnov, E. Tikhonenko, N. Voytishin, A. Zarubin

Petersburg Nuclear Physics Institute, Gatchina (St. Petersburg), Russia
L. Chtchipounov, V. Golovtsov, Y. Ivanov, V. Kim[39], E. Kuznetsova[40], V. Murzin, V. Oreshkin, V. Sulimov, A. Vorobyev

Institute for Nuclear Research, Moscow, Russia
Yu. Andreev, A. Dermenev, S. Gninenko, N. Golubev, A. Karneyeu, M. Kirsanov, N. Krasnikov, A. Pashenkov, D. Tlisov, A. Toropin

Institute for Theoretical and Experimental Physics, Moscow, Russia
V. Epshteyn, V. Gavrilov, N. Lychkovskaya, V. Popov, I. Pozdnyakov, G. Safronov, A. Spiridonov, M. Toms, E. Vlasov, A. Zhokin

Moscow Institute of Physics and Technology
A. Bylinkin[38]

National Research Nuclear University 'Moscow Engineering Physics Institute' (MEPhI), Moscow, Russia
M. Chadeeva[41], E. Popova, E. Tarkovskii

P.N. Lebedev Physical Institute, Moscow, Russia
V. Andreev, M. Azarkin[38], I. Dremin[38], M. Kirakosyan, A. Leonidov[38], S.V. Rusakov, A. Terkulov

Skobeltsyn Institute of Nuclear Physics, Lomonosov Moscow State University, Moscow, Russia
A. Baskakov, A. Belyaev, E. Boos, M. Dubinin[42], L. Dudko, A. Ershov, A. Gribushin, V. Klyukhin, O. Kodolova, I. Lokhtin, I. Miagkov, S. Obraztsov, S. Petrushanko, V. Savrin, A. Snigirev

Novosibirsk State University (NSU), Novosibirsk, Russia
V. Blinov[43], Y.Skovpen[43]

State Research Center of Russian Federation, Institute for High Energy Physics, Protvino, Russia
I. Azhgirey, I. Bayshev, S. Bitioukov, D. Elumakhov, V. Kachanov, A. Kalinin, D. Konstantinov, V. Krychkine, V. Petrov, R. Ryutin, A. Sobol, S. Troshin, N. Tyurin, A. Uzunian, A. Volkov

University of Belgrade, Faculty of Physics and Vinca Institute of Nuclear Sciences, Belgrade, Serbia

P. Adzic[44], P. Cirkovic, D. Devetak, M. Dordevic, J. Milosevic, V. Rekovic

Centro de Investigaciones Energéticas Medioambientales y Tecnológicas (CIEMAT), Madrid, Spain

J. Alcaraz Maestre, M. Barrio Luna, E. Calvo, M. Cerrada, M. Chamizo Llatas, N. Colino, B. De La Cruz, A. Delgado Peris, A. Escalante Del Valle, C. Fernandez Bedoya, J.P. Fernández Ramos, J. Flix, M.C. Fouz, P. Garcia-Abia, O. Gonzalez Lopez, S. Goy Lopez, J.M. Hernandez, M.I. Josa, E. Navarro De Martino, A. Pérez-Calero Yzquierdo, J. Puerta Pelayo, A. Quintario Olmeda, I. Redondo, L. Romero, M.S. Soares

Universidad Autónoma de Madrid, Madrid, Spain

J.F. de Trocóniz, M. Missiroli, D. Moran

Universidad de Oviedo, Oviedo, Spain

J. Cuevas, J. Fernandez Menendez, I. Gonzalez Caballero, J.R. González Fernández, E. Palencia Cortezon, S. Sanchez Cruz, I. Suárez Andrés, J.M. Vizan Garcia

Instituto de Física de Cantabria (IFCA), CSIC-Universidad de Cantabria, Santander, Spain

I.J. Cabrillo, A. Calderon, J.R. Castiñeiras De Saa, E. Curras, M. Fernandez, J. Garcia-Ferrero, G. Gomez, A. Lopez Virto, J. Marco, C. Martinez Rivero, F. Matorras, J. Piedra Gomez, T. Rodrigo, A. Ruiz-Jimeno, L. Scodellaro, N. Trevisani, I. Vila, R. Vilar Cortabitarte

CERN, European Organization for Nuclear Research, Geneva, Switzerland

D. Abbaneo, E. Auffray, G. Auzinger, M. Bachtis, P. Baillon, A.H. Ball, D. Barney, P. Bloch, A. Bocci, A. Bonato, C. Botta, T. Camporesi, R. Castello, M. Cepeda, G. Cerminara, M. D'Alfonso, D. d'Enterria, A. Dabrowski, V. Daponte, A. David, M. De Gruttola, A. De Roeck, E. Di Marco[45], M. Dobson, B. Dorney, T. du Pree, D. Duggan, M. Dünser, N. Dupont, A. Elliott-Peisert, S. Fartoukh, G. Franzoni, J. Fulcher, W. Funk, D. Gigi, K. Gill, M. Girone, F. Glege, D. Gulhan, S. Gundacker, M. Guthoff, J. Hammer, P. Harris, J. Hegeman, V. Innocente, P. Janot, H. Kirschenmann, V. Knünz, A. Kornmayer[16], M.J. Kortelainen, K. Kousouris, M. Krammer[1], P. Lecoq, C. Lourenço, M.T. Lucchini, L. Malgeri, M. Mannelli, A. Martelli, F. Meijers, J.A. Merlin, S. Mersi, E. Meschi, F. Moortgat, S. Morovic, M. Mulders, H. Neugebauer, S. Orfanelli, L. Orsini, L. Pape, E. Perez, M. Peruzzi, A. Petrilli, G. Petrucciani, A. Pfeiffer, M. Pierini, A. Racz, T. Reis, G. Rolandi[46], M. Rovere, M. Ruan, H. Sakulin, J.B. Sauvan, C. Schäfer, C. Schwick, M. Seidel, A. Sharma, P. Silva, P. Sphicas[47], J. Steggemann, M. Stoye, Y. Takahashi, M. Tosi, D. Treille, A. Triossi, A. Tsirou, V. Veckalns[48], G.I. Veres[21], N. Wardle, A. Zagozdzinska[36], W.D. Zeuner

Paul Scherrer Institut, Villigen, Switzerland

W. Bertl, K. Deiters, W. Erdmann, R. Horisberger, Q. Ingram, H.C. Kaestli, D. Kotlinski, U. Langenegger, T. Rohe

Institute for Particle Physics, ETH Zurich, Zurich, Switzerland

F. Bachmair, L. Bäni, L. Bianchini, B. Casal, G. Dissertori, M. Dittmar, M. Donegà, P. Eller, C. Grab, C. Heidegger, D. Hits, J. Hoss, G. Kasieczka, P. Lecomte[†], W. Lustermann, B. Mangano, M. Marionneau, P. Martinez Ruiz del Arbol, M. Masciovecchio, M.T. Meinhard, D. Meister, F. Micheli, P. Musella, F. Nessi-Tedaldi, F. Pandolfi, J. Pata, F. Pauss, G. Perrin, L. Perrozzi, M. Quittnat, M. Rossini, M. Schönenberger, A. Starodumov[49], V.R. Tavolaro, K. Theofilatos, R. Wallny

Universität Zürich, Zurich, Switzerland
T.K. Aarrestad, C. Amsler[50], L. Caminada, M.F. Canelli, A. De Cosa, C. Galloni, A. Hinzmann, T. Hreus, B. Kilminster, C. Lange, J. Ngadiuba, D. Pinna, G. Rauco, P. Robmann, D. Salerno, Y. Yang

National Central University, Chung-Li, Taiwan
V. Candelise, T.H. Doan, Sh. Jain, R. Khurana, M. Konyushikhin, C.M. Kuo, W. Lin, Y.J. Lu, A. Pozdnyakov, S.S. Yu

National Taiwan University (NTU), Taipei, Taiwan
Arun Kumar, P. Chang, Y.H. Chang, Y.W. Chang, Y. Chao, K.F. Chen, P.H. Chen, C. Dietz, F. Fiori, W.-S. Hou, Y. Hsiung, Y.F. Liu, R.-S. Lu, M. Miñano Moya, E. Paganis, A. Psallidas, J.f. Tsai, Y.M. Tzeng

Chulalongkorn University, Faculty of Science, Department of Physics, Bangkok, Thailand
B. Asavapibhop, G. Singh, N. Srimanobhas, N. Suwonjandee

Cukurova University, Adana, Turkey
M.N. Bakirci[51], S. Damarseckin, Z.S. Demiroglu, C. Dozen, E. Eskut, S. Girgis, G. Gokbulut, Y. Guler, E. Gurpinar, I. Hos, E.E. Kangal[52], O. Kara, U. Kiminsu, M. Oglakci, G. Onengut[53], K. Ozdemir[54], S. Ozturk[51], A. Polatoz, D. Sunar Cerci[55], S. Turkcapar, I.S. Zorbakir, C. Zorbilmez

Middle East Technical University, Physics Department, Ankara, Turkey
B. Bilin, S. Bilmis, B. Isildak[56], G. Karapinar[57], K. Ocalan[58], M. Yalvac, M. Zeyrek

Bogazici University, Istanbul, Turkey
E. Gülmez, M. Kaya[59], O. Kaya[60], E.A. Yetkin[61], T. Yetkin[62]

Istanbul Technical University, Istanbul, Turkey
A. Cakir, K. Cankocak, S. Sen[63]

Institute for Scintillation Materials of National Academy of Science of Ukraine, Kharkov, Ukraine
B. Grynyov

National Scientific Center, Kharkov Institute of Physics and Technology, Kharkov, Ukraine
L. Levchuk, P. Sorokin

University of Bristol, Bristol, United Kingdom
R. Aggleton, F. Ball, L. Beck, J.J. Brooke, D. Burns, E. Clement, D. Cussans, H. Flacher, J. Goldstein, M. Grimes, G.P. Heath, H.F. Heath, J. Jacob, L. Kreczko, C. Lucas, D.M. Newbold[64], S. Paramesvaran, A. Poll, T. Sakuma, S. Seif El Nasr-storey, D. Smith, V.J. Smith

Rutherford Appleton Laboratory, Didcot, United Kingdom
D. Barducci, K.W. Bell, A. Belyaev[65], C. Brew, R.M. Brown, L. Calligaris, D. Cieri, D.J.A. Cockerill, J.A. Coughlan, K. Harder, S. Harper, E. Olaiya, D. Petyt, C.H. Shepherd-Themistocleous, A. Thea, I.R. Tomalin, T. Williams

Imperial College, London, United Kingdom
M. Baber, R. Bainbridge, O. Buchmuller, A. Bundock, D. Burton, S. Casasso, M. Citron, D. Colling, L. Corpe, P. Dauncey, G. Davies, A. De Wit, M. Della Negra, R. Di Maria, P. Dunne, A. Elwood, D. Futyan, Y. Haddad, G. Hall, G. Iles, T. James, R. Lane, C. Laner, R. Lucas[64], L. Lyons, A.-M. Magnan, S. Malik, L. Mastrolorenzo, J. Nash, A. Nikitenko[49], J. Pela, B. Penning,

M. Pesaresi, D.M. Raymond, A. Richards, A. Rose, C. Seez, S. Summers, A. Tapper, K. Uchida, M. Vazquez Acosta[66], T. Virdee[16], J. Wright, S.C. Zenz

Brunel University, Uxbridge, United Kingdom
J.E. Cole, P.R. Hobson, A. Khan, P. Kyberd, D. Leslie, I.D. Reid, P. Symonds, L. Teodorescu, M. Turner

Baylor University, Waco, USA
A. Borzou, K. Call, J. Dittmann, K. Hatakeyama, H. Liu, N. Pastika

The University of Alabama, Tuscaloosa, USA
O. Charaf, S.I. Cooper, C. Henderson, P. Rumerio, C. West

Boston University, Boston, USA
D. Arcaro, A. Avetisyan, T. Bose, D. Gastler, D. Rankin, C. Richardson, J. Rohlf, L. Sulak, D. Zou

Brown University, Providence, USA
G. Benelli, E. Berry, D. Cutts, A. Garabedian, J. Hakala, U. Heintz, J.M. Hogan, O. Jesus, E. Laird, G. Landsberg, Z. Mao, M. Narain, S. Piperov, S. Sagir, E. Spencer, R. Syarif

University of California, Davis, Davis, USA
R. Breedon, G. Breto, D. Burns, M. Calderon De La Barca Sanchez, S. Chauhan, M. Chertok, J. Conway, R. Conway, P.T. Cox, R. Erbacher, C. Flores, G. Funk, M. Gardner, W. Ko, R. Lander, C. Mclean, M. Mulhearn, D. Pellett, J. Pilot, F. Ricci-Tam, S. Shalhout, J. Smith, M. Squires, D. Stolp, M. Tripathi, S. Wilbur, R. Yohay

University of California, Los Angeles, USA
R. Cousins, P. Everaerts, A. Florent, J. Hauser, M. Ignatenko, D. Saltzberg, E. Takasugi, V. Valuev, M. Weber

University of California, Riverside, Riverside, USA
K. Burt, R. Clare, J. Ellison, J.W. Gary, G. Hanson, J. Heilman, P. Jandir, E. Kennedy, F. Lacroix, O.R. Long, M. Olmedo Negrete, M.I. Paneva, A. Shrinivas, H. Wei, S. Wimpenny, B. R. Yates

University of California, San Diego, La Jolla, USA
J.G. Branson, G.B. Cerati, S. Cittolin, M. Derdzinski, R. Gerosa, A. Holzner, D. Klein, V. Krutelyov, J. Letts, I. Macneill, D. Olivito, S. Padhi, M. Pieri, M. Sani, V. Sharma, S. Simon, M. Tadel, A. Vartak, S. Wasserbaech[67], C. Welke, J. Wood, F. Würthwein, A. Yagil, G. Zevi Della Porta

University of California, Santa Barbara - Department of Physics, Santa Barbara, USA
R. Bhandari, J. Bradmiller-Feld, C. Campagnari, A. Dishaw, V. Dutta, K. Flowers, M. Franco Sevilla, P. Geffert, C. George, F. Golf, L. Gouskos, J. Gran, R. Heller, J. Incandela, N. Mccoll, S.D. Mullin, A. Ovcharova, J. Richman, D. Stuart, I. Suarez, J. Yoo

California Institute of Technology, Pasadena, USA
D. Anderson, A. Apresyan, J. Bendavid, A. Bornheim, J. Bunn, Y. Chen, J. Duarte, J.M. Lawhorn, A. Mott, H.B. Newman, C. Pena, M. Spiropulu, J.R. Vlimant, S. Xie, R.Y. Zhu

Carnegie Mellon University, Pittsburgh, USA
M.B. Andrews, V. Azzolini, T. Ferguson, M. Paulini, J. Russ, M. Sun, H. Vogel, I. Vorobiev

University of Colorado Boulder, Boulder, USA
J.P. Cumalat, W.T. Ford, F. Jensen, A. Johnson, M. Krohn, T. Mulholland, K. Stenson, S.R. Wagner

Cornell University, Ithaca, USA
J. Alexander, J. Chaves, J. Chu, S. Dittmer, K. Mcdermott, N. Mirman, G. Nicolas Kaufman, J.R. Patterson, A. Rinkevicius, A. Ryd, L. Skinnari, L. Soffi, S.M. Tan, Z. Tao, J. Thom, J. Tucker, P. Wittich, M. Zientek

Fairfield University, Fairfield, USA
D. Winn

Fermi National Accelerator Laboratory, Batavia, USA
S. Abdullin, M. Albrow, G. Apollinari, S. Banerjee, L.A.T. Bauerdick, A. Beretvas, J. Berryhill, P.C. Bhat, G. Bolla, K. Burkett, J.N. Butler, H.W.K. Cheung, F. Chlebana, S. Cihangir†, M. Cremonesi, V.D. Elvira, I. Fisk, J. Freeman, E. Gottschalk, L. Gray, D. Green, S. Grünendahl, O. Gutsche, D. Hare, R.M. Harris, S. Hasegawa, J. Hirschauer, Z. Hu, B. Jayatilaka, S. Jindariani, M. Johnson, U. Joshi, B. Klima, B. Kreis, S. Lammel, J. Linacre, D. Lincoln, R. Lipton, T. Liu, R. Lopes De Sá, J. Lykken, K. Maeshima, N. Magini, J.M. Marraffino, S. Maruyama, D. Mason, P. McBride, P. Merkel, S. Mrenna, S. Nahn, C. Newman-Holmes†, V. O'Dell, K. Pedro, O. Prokofyev, G. Rakness, L. Ristori, E. Sexton-Kennedy, A. Soha, W.J. Spalding, L. Spiegel, S. Stoynev, N. Strobbe, L. Taylor, S. Tkaczyk, N.V. Tran, L. Uplegger, E.W. Vaandering, C. Vernieri, M. Verzocchi, R. Vidal, M. Wang, H.A. Weber, A. Whitbeck

University of Florida, Gainesville, USA
D. Acosta, P. Avery, P. Bortignon, D. Bourilkov, A. Brinkerhoff, A. Carnes, M. Carver, D. Curry, S. Das, R.D. Field, I.K. Furic, J. Konigsberg, A. Korytov, P. Ma, K. Matchev, H. Mei, P. Milenovic[68], G. Mitselmakher, D. Rank, L. Shchutska, D. Sperka, L. Thomas, J. Wang, S. Wang, J. Yelton

Florida International University, Miami, USA
S. Linn, P. Markowitz, G. Martinez, J.L. Rodriguez

Florida State University, Tallahassee, USA
A. Ackert, J.R. Adams, T. Adams, A. Askew, S. Bein, B. Diamond, S. Hagopian, V. Hagopian, K.F. Johnson, A. Khatiwada, H. Prosper, A. Santra, M. Weinberg

Florida Institute of Technology, Melbourne, USA
M.M. Baarmand, V. Bhopatkar, S. Colafranceschi[69], M. Hohlmann, D. Noonan, T. Roy, F. Yumiceva

University of Illinois at Chicago (UIC), Chicago, USA
M.R. Adams, L. Apanasevich, D. Berry, R.R. Betts, I. Bucinskaite, R. Cavanaugh, O. Evdokimov, L. Gauthier, C.E. Gerber, D.J. Hofman, P. Kurt, C. O'Brien, I.D. Sandoval Gonzalez, P. Turner, N. Varelas, H. Wang, Z. Wu, M. Zakaria, J. Zhang

The University of Iowa, Iowa City, USA
B. Bilki[70], W. Clarida, K. Dilsiz, S. Durgut, R.P. Gandrajula, M. Haytmyradov, V. Khristenko, J.-P. Merlo, H. Mermerkaya[71], A. Mestvirishvili, A. Moeller, J. Nachtman, H. Ogul, Y. Onel, F. Ozok[72], A. Penzo, C. Snyder, E. Tiras, J. Wetzel, K. Yi

Johns Hopkins University, Baltimore, USA
I. Anderson, B. Blumenfeld, A. Cocoros, N. Eminizer, D. Fehling, L. Feng, A.V. Gritsan, P. Maksimovic, M. Osherson, J. Roskes, U. Sarica, M. Swartz, M. Xiao, Y. Xin, C. You

The University of Kansas, Lawrence, USA
A. Al-bataineh, P. Baringer, A. Bean, S. Boren, J. Bowen, C. Bruner, J. Castle, L. Forthomme,

R.P. Kenny III, A. Kropivnitskaya, D. Majumder, W. Mcbrayer, M. Murray, S. Sanders, R. Stringer, J.D. Tapia Takaki, Q. Wang

Kansas State University, Manhattan, USA
A. Ivanov, K. Kaadze, S. Khalil, M. Makouski, Y. Maravin, A. Mohammadi, L.K. Saini, N. Skhirtladze, S. Toda

Lawrence Livermore National Laboratory, Livermore, USA
F. Rebassoo, D. Wright

University of Maryland, College Park, USA
C. Anelli, A. Baden, O. Baron, A. Belloni, B. Calvert, S.C. Eno, C. Ferraioli, J.A. Gomez, N.J. Hadley, S. Jabeen, R.G. Kellogg, T. Kolberg, J. Kunkle, Y. Lu, A.C. Mignerey, Y.H. Shin, A. Skuja, M.B. Tonjes, S.C. Tonwar

Massachusetts Institute of Technology, Cambridge, USA
D. Abercrombie, B. Allen, A. Apyan, R. Barbieri, A. Baty, R. Bi, K. Bierwagen, S. Brandt, W. Busza, I.A. Cali, Z. Demiragli, L. Di Matteo, G. Gomez Ceballos, M. Goncharov, D. Hsu, Y. Iiyama, G.M. Innocenti, M. Klute, D. Kovalskyi, K. Krajczar, Y.S. Lai, Y.-J. Lee, A. Levin, P.D. Luckey, A.C. Marini, C. Mcginn, C. Mironov, S. Narayanan, X. Niu, C. Paus, C. Roland, G. Roland, J. Salfeld-Nebgen, G.S.F. Stephans, K. Sumorok, K. Tatar, M. Varma, D. Velicanu, J. Veverka, J. Wang, T.W. Wang, B. Wyslouch, M. Yang, V. Zhukova

University of Minnesota, Minneapolis, USA
A.C. Benvenuti, R.M. Chatterjee, A. Evans, A. Finkel, A. Gude, P. Hansen, S. Kalafut, S.C. Kao, Y. Kubota, Z. Lesko, J. Mans, S. Nourbakhsh, N. Ruckstuhl, R. Rusack, N. Tambe, J. Turkewitz

University of Mississippi, Oxford, USA
J.G. Acosta, S. Oliveros

University of Nebraska-Lincoln, Lincoln, USA
E. Avdeeva, R. Bartek, K. Bloom, D.R. Claes, A. Dominguez, C. Fangmeier, R. Gonzalez Suarez, R. Kamalieddin, I. Kravchenko, A. Malta Rodrigues, F. Meier, J. Monroy, J.E. Siado, G.R. Snow, B. Stieger

State University of New York at Buffalo, Buffalo, USA
M. Alyari, J. Dolen, J. George, A. Godshalk, C. Harrington, I. Iashvili, J. Kaisen, A. Kharchilava, A. Kumar, A. Parker, S. Rappoccio, B. Roozbahani

Northeastern University, Boston, USA
G. Alverson, E. Barberis, D. Baumgartel, A. Hortiangtham, A. Massironi, D.M. Morse, D. Nash, T. Orimoto, R. Teixeira De Lima, D. Trocino, R.-J. Wang, D. Wood

Northwestern University, Evanston, USA
S. Bhattacharya, K.A. Hahn, A. Kubik, A. Kumar, J.F. Low, N. Mucia, N. Odell, B. Pollack, M.H. Schmitt, K. Sung, M. Trovato, M. Velasco

University of Notre Dame, Notre Dame, USA
N. Dev, M. Hildreth, K. Hurtado Anampa, C. Jessop, D.J. Karmgard, N. Kellams, K. Lannon, N. Marinelli, F. Meng, C. Mueller, Y. Musienko[37], M. Planer, A. Reinsvold, R. Ruchti, G. Smith, S. Taroni, M. Wayne, M. Wolf, A. Woodard

The Ohio State University, Columbus, USA
J. Alimena, L. Antonelli, J. Brinson, B. Bylsma, L.S. Durkin, S. Flowers, B. Francis, A. Hart, C. Hill, R. Hughes, W. Ji, B. Liu, W. Luo, D. Puigh, B.L. Winer, H.W. Wulsin

Princeton University, Princeton, USA
S. Cooperstein, O. Driga, P. Elmer, J. Hardenbrook, P. Hebda, D. Lange, J. Luo, D. Marlow,
T. Medvedeva, K. Mei, M. Mooney, J. Olsen, C. Palmer, P. Piroué, D. Stickland, C. Tully,
A. Zuranski

University of Puerto Rico, Mayaguez, USA
S. Malik

Purdue University, West Lafayette, USA
A. Barker, V.E. Barnes, S. Folgueras, L. Gutay, M.K. Jha, M. Jones, A.W. Jung, K. Jung,
D.H. Miller, N. Neumeister, X. Shi, J. Sun, A. Svyatkovskiy, F. Wang, W. Xie, L. Xu

Purdue University Calumet, Hammond, USA
N. Parashar, J. Stupak

Rice University, Houston, USA
A. Adair, B. Akgun, Z. Chen, K.M. Ecklund, F.J.M. Geurts, M. Guilbaud, W. Li, B. Michlin,
M. Northup, B.P. Padley, R. Redjimi, J. Roberts, J. Rorie, Z. Tu, J. Zabel

University of Rochester, Rochester, USA
B. Betchart, A. Bodek, P. de Barbaro, R. Demina, Y.t. Duh, T. Ferbel, M. Galanti, A. Garcia-
Bellido, J. Han, O. Hindrichs, A. Khukhunaishvili, K.H. Lo, P. Tan, M. Verzetti

Rutgers, The State University of New Jersey, Piscataway, USA
A. Agapitos, J.P. Chou, E. Contreras-Campana, Y. Gershtein, T.A. Gómez Espinosa,
E. Halkiadakis, M. Heindl, D. Hidas, E. Hughes, S. Kaplan, R. Kunnawalkam Elayavalli,
S. Kyriacou, A. Lath, K. Nash, H. Saka, S. Salur, S. Schnetzer, D. Sheffield, S. Somalwar, R. Stone,
S. Thomas, P. Thomassen, M. Walker

University of Tennessee, Knoxville, USA
M. Foerster, J. Heideman, G. Riley, K. Rose, S. Spanier, K. Thapa

Texas A&M University, College Station, USA
O. Bouhali[73], A. Celik, M. Dalchenko, M. De Mattia, A. Delgado, S. Dildick, R. Eusebi,
J. Gilmore, T. Huang, E. Juska, T. Kamon[74], R. Mueller, Y. Pakhotin, R. Patel, A. Perloff,
L. Perniè, D. Rathjens, A. Rose, A. Safonov, A. Tatarinov, K.A. Ulmer

Texas Tech University, Lubbock, USA
N. Akchurin, C. Cowden, J. Damgov, F. De Guio, C. Dragoiu, P.R. Dudero, J. Faulkner,
S. Kunori, K. Lamichhane, S.W. Lee, T. Libeiro, S. Undleeb, I. Volobouev, Z. Wang

Vanderbilt University, Nashville, USA
A.G. Delannoy, S. Greene, A. Gurrola, R. Janjam, W. Johns, C. Maguire, A. Melo, H. Ni,
P. Sheldon, S. Tuo, J. Velkovska, Q. Xu

University of Virginia, Charlottesville, USA
M.W. Arenton, P. Barria, B. Cox, J. Goodell, R. Hirosky, A. Ledovskoy, H. Li, C. Neu,
T. Sinthuprasith, Y. Wang, E. Wolfe, F. Xia

Wayne State University, Detroit, USA
C. Clarke, R. Harr, P.E. Karchin, P. Lamichhane, J. Sturdy

University of Wisconsin - Madison, Madison, WI, USA
D.A. Belknap, S. Dasu, L. Dodd, S. Duric, B. Gomber, M. Grothe, M. Herndon, A. Hervé,
P. Klabbers, A. Lanaro, A. Levine, K. Long, R. Loveless, I. Ojalvo, T. Perry, G.A. Pierro,
G. Polese, T. Ruggles, A. Savin, A. Sharma, N. Smith, W.H. Smith, D. Taylor, N. Woods

†: Deceased
1: Also at Vienna University of Technology, Vienna, Austria
2: Also at State Key Laboratory of Nuclear Physics and Technology, Peking University, Beijing, China
3: Also at Institut Pluridisciplinaire Hubert Curien, Université de Strasbourg, Université de Haute Alsace Mulhouse, CNRS/IN2P3, Strasbourg, France
4: Also at Universidade Estadual de Campinas, Campinas, Brazil
5: Also at Universidade Federal de Pelotas, Pelotas, Brazil
6: Also at Université Libre de Bruxelles, Bruxelles, Belgium
7: Also at Deutsches Elektronen-Synchrotron, Hamburg, Germany
8: Also at Joint Institute for Nuclear Research, Dubna, Russia
9: Also at Helwan University, Cairo, Egypt
10: Now at Zewail City of Science and Technology, Zewail, Egypt
11: Now at Fayoum University, El-Fayoum, Egypt
12: Also at British University in Egypt, Cairo, Egypt
13: Now at Ain Shams University, Cairo, Egypt
14: Also at Université de Haute Alsace, Mulhouse, France
15: Also at Skobeltsyn Institute of Nuclear Physics, Lomonosov Moscow State University, Moscow, Russia
16: Also at CERN, European Organization for Nuclear Research, Geneva, Switzerland
17: Also at RWTH Aachen University, III. Physikalisches Institut A, Aachen, Germany
18: Also at University of Hamburg, Hamburg, Germany
19: Also at Brandenburg University of Technology, Cottbus, Germany
20: Also at Institute of Nuclear Research ATOMKI, Debrecen, Hungary
21: Also at MTA-ELTE Lendület CMS Particle and Nuclear Physics Group, Eötvös Loránd University, Budapest, Hungary
22: Also at University of Debrecen, Debrecen, Hungary
23: Also at Indian Institute of Science Education and Research, Bhopal, India
24: Also at Institute of Physics, Bhubaneswar, India
25: Also at University of Visva-Bharati, Santiniketan, India
26: Also at University of Ruhuna, Matara, Sri Lanka
27: Also at Isfahan University of Technology, Isfahan, Iran
28: Also at University of Tehran, Department of Engineering Science, Tehran, Iran
29: Also at Yazd University, Yazd, Iran
30: Also at Plasma Physics Research Center, Science and Research Branch, Islamic Azad University, Tehran, Iran
31: Also at Università degli Studi di Siena, Siena, Italy
32: Also at Purdue University, West Lafayette, USA
33: Also at International Islamic University of Malaysia, Kuala Lumpur, Malaysia
34: Also at Malaysian Nuclear Agency, MOSTI, Kajang, Malaysia
35: Also at Consejo Nacional de Ciencia y Tecnología, Mexico city, Mexico
36: Also at Warsaw University of Technology, Institute of Electronic Systems, Warsaw, Poland
37: Also at Institute for Nuclear Research, Moscow, Russia
38: Now at National Research Nuclear University 'Moscow Engineering Physics Institute' (MEPhI), Moscow, Russia
39: Also at St. Petersburg State Polytechnical University, St. Petersburg, Russia
40: Also at University of Florida, Gainesville, USA
41: Also at P.N. Lebedev Physical Institute, Moscow, Russia
42: Also at California Institute of Technology, Pasadena, USA

43: Also at Budker Institute of Nuclear Physics, Novosibirsk, Russia
44: Also at Faculty of Physics, University of Belgrade, Belgrade, Serbia
45: Also at INFN Sezione di Roma; Università di Roma, Roma, Italy
46: Also at Scuola Normale e Sezione dell'INFN, Pisa, Italy
47: Also at National and Kapodistrian University of Athens, Athens, Greece
48: Also at Riga Technical University, Riga, Latvia
49: Also at Institute for Theoretical and Experimental Physics, Moscow, Russia
50: Also at Albert Einstein Center for Fundamental Physics, Bern, Switzerland
51: Also at Gaziosmanpasa University, Tokat, Turkey
52: Also at Mersin University, Mersin, Turkey
53: Also at Cag University, Mersin, Turkey
54: Also at Piri Reis University, Istanbul, Turkey
55: Also at Adiyaman University, Adiyaman, Turkey
56: Also at Ozyegin University, Istanbul, Turkey
57: Also at Izmir Institute of Technology, Izmir, Turkey
58: Also at Necmettin Erbakan University, Konya, Turkey
59: Also at Marmara University, Istanbul, Turkey
60: Also at Kafkas University, Kars, Turkey
61: Also at Istanbul Bilgi University, Istanbul, Turkey
62: Also at Yildiz Technical University, Istanbul, Turkey
63: Also at Hacettepe University, Ankara, Turkey
64: Also at Rutherford Appleton Laboratory, Didcot, United Kingdom
65: Also at School of Physics and Astronomy, University of Southampton, Southampton, United Kingdom
66: Also at Instituto de Astrofísica de Canarias, La Laguna, Spain
67: Also at Utah Valley University, Orem, USA
68: Also at University of Belgrade, Faculty of Physics and Vinca Institute of Nuclear Sciences, Belgrade, Serbia
69: Also at Facoltà Ingegneria, Università di Roma, Roma, Italy
70: Also at Argonne National Laboratory, Argonne, USA
71: Also at Erzincan University, Erzincan, Turkey
72: Also at Mimar Sinan University, Istanbul, Istanbul, Turkey
73: Also at Texas A&M University at Qatar, Doha, Qatar
74: Also at Kyungpook National University, Daegu, Korea